

SEP 20 1971

ATTENUATION AND DOSE MEASUREMENTS
USING 14.1 MEV NEUTRONS

Ö.Dalli

A THESIS

in

Physics

Presented in Partial Fulfillment of the Requirements for
Degree of Master of Science at
Sir George Williams University

June, 1970

ABSTRACT

ATTENUATION AND DOSE MEASUREMENTS

USING 14.1 MEV NEUTRONS

by

Ö.Dalli

The attenuation of a fast neutron beam of 14.1 MeV in steel, paraffin, borated paraffin, borated water lead and in combinations of these materials, is studied and the absorbed dose rates through these materials in a tissue-equivalent material are determined. It is shown that while steel is one of the best materials for attenuating the primary neutrons, it is advantageous to add paraffin or borated paraffin to attenuate slowed down neutrons scattered from the steel and from the other materials around the target. Data are given for the radiation emerging from shields using various combinations of these materials.

TABLE OF CONTENTS

	Page
ACKNOWLEDGEMENTS	
ABSTRACT	1
CHAPTER I INTRODUCTION	2
1.1 Brief history	2
1.2 The importance of neutrons in radiobiology	3
CHAPTER II MECHANISM OF ENERGY DEPOSITION	5
2.1 General	5
2.2 Production of directly ionizing particles	6
2.2.1 X- and gamma-rays	6
2.2.2 Neutrons	6
2.3 Energy deposition by directly ionizing particles	8
2.4 Macroscopic treatment of radiation absorption	10
CHAPTER III ABSORBED DOSE OF NEUTRONS	11
3.1 Concepts and units of radiation dosimetry	11
3.2 Interactions between neutrons and tissue	20
3.3 Method of dosimetry	23

TABLE OF CONTENTS (continued)

3.3.1	General	23
3.3.2	Tissue-equivalent chambers	24
3.3.3	Relative contribution of gas and wall of the chamber	25
CHAPTER IV	OPERATION AND YIELD OF NEUTRON GENERATOR	28
4.1	Nuclear reactions of neutron generator	28
4.2	Operation and design of neutron generator	28
4.2.1	Ion source and gap lens	29
4.2.2	Accelerating tube	31
4.2.3	Drift tube and target assembly	34
4.3	Shielding of neutrons	35
CHAPTER V	EXPERIMENTAL PROCEDURE' RESULTS AND DISCUSSION	40
5.1	The tissue-equivalent ionization chamber	40
5.2	Shielding of the generator	42
5.3	Experimental procedure	45
5.4	Determination of the absorbed dose	46
5.5	Attenuation results and discussion	49
CHAPTER VI	CONCLUSION	66
REFERENCES		68

ACKNOWLEDGEMENTS

The author wishes to thank Dr. D. Charlton for suggesting this thesis problem and for his direction of the research work reported here.

The author also acknowledges the assistance of Mr. J. Loustau in construction of the ionization chamber. A special note of thanks to Mr. A. Christodouloupolos for his helpful assistance during this work.

The facilities offered by Dr. W. R. Raudorf, chairman of the physics department, are greatly appreciated.

CHAPTER I

INTRODUCTION

1.1 Brief history

Physics opened a new area in biology with the discovery of X-rays by Roentgen in 1895. This was followed closely by the discovery of natural radioactivity by Becquerel in 1896. Each unwittingly performed biological experiments. Roentgen made visible the bones of his hand by interposing it between his vacuum tube and an improvised fluorescent screen: the Curies had succeeded in extracting and purifying radium by 1898.

Roentgen's experience gave impetus to the development of diagnostic radiology, while Becquerel's skin damage led to an earnest medical investigation of the effects of natural radioactivity. In time the latter resulted in therapeutic applications not only of isotopes but also of rays from man-made generators.

The growth of therapeutic and diagnostic departments has often been administratively separate because of the historical independence of interest. Furthermore, operators of diagnostic equipment have not always appreciated the damaging effects of the rays. The time interval between cause and effect has contributed to this unfortunate situation. Occasionally ignorance of or indifference to mutagenic potency is still encountered.

Except for attention by geneticists, sustained general interest in radiobiology seems to be chiefly an aftermath of the atomic explosions of 1945. Full appreciation of even the genetic investigations was delayed until after this significant date. Although Muller (Muller 1927) reported his convincing experiments in 1927, it was not until 1946 that public recognition came with the award of the Nobel Prize. During the development of the Atom Bomb and subsequent increase of public interest in nuclear reactor operations, national and private laboratories devoted tremendous resources to the study of basic and applied aspects of atomic physics.

The cause of radiobiology is paralleled by the change in attitude toward uranium. Before the Atomic Age, uranium was said to have no important uses. It was many years after its first isolation that uranium suddenly became one of the most important elements.

The stimulus to radiobiology from advances in atomic physics cannot be overestimated. There are intangible aspects in addition to the tangible advantages of a plentiful supply of radioactive isotopes, measuring instruments, and generators.

1.2 The importance of neutrons in radiobiology .

The objective of the dosimetry of neutrons must usually be more than a mere determination of the absorbed dose. The biological effectiveness of electromagnetic radiation varies by perhaps 5 % over the entire spectrum commonly

available (say from 10 keV to 10 MeV), but radiations such as neutrons and heavy charged particles which lose energies at high rates (>10 keV/ μ) show considerable variability of biological effectiveness (by factors of up to 10) depending on radiation energy type and biological system.

The use of these heavy charged particles in radiotherapy is quite impossible because of accelerating difficulties. For example, the total irradiation of a biological object having a diameter of 15 cm with charged particles with rate of energy loss of 100 keV/ μ requires a particle accelerator capable of producing heavy charged particles with an energy of about 10^4 MeV. These accelerating machines are not available up to the present.

The possibility of using neutrons for radiotherapy of tumors is one of the important parts of this field. Many tumors may contain anoxic cells. For electromagnetic radiation such as X- or gamma-rays these anoxic cells are much less sensitive to irradiation than well oxygenated cells and, therefore, more difficult to treat by conventional means. This difference in sensitivity is smaller if radiation with a higher rate of energy loss is used. The combination of moderately good penetration in tissue and the low oxygen enhancement ratio makes the use of fast neutrons most suitable for radiotherapy.

CHAPTER II

MECHANISM OF ENERGY DEPOSITION

2.1 General

To understand how radiation is absorbed in matter, it is desirable to know the interaction of radiation with matter.

An ionizing radiation is any radiation consisting of directly ionizing particles, or indirectly ionizing particles, or a mixture of both. Directly ionizing particles are defined as charged particles (electrons, protons, alpha-particles, etc.) having sufficient energy to produce ionization by collision and indirectly ionizing particles are defined as uncharged particles (neutrons, photons, etc.) which can liberate directly ionizing particles or can initiate a nuclear transformation (ICRU 1962).

Regardless of the nature of incident radiation, transfer of energy to the medium devolves ultimately on the interaction of more or less swiftly moving charged particles. In other words only charged particles can deposit energy.

Absorption in matter of any such radiation from sources which may be external or internal, gives rise to electronically excited and ionized molecules of a variety of types, and on a submicroscopic scale drastically inhomogeneous spatial arrangements. These activated molecules, which are often called "primary products" are usually extremely un-

stable, and initiate the following sequence of events: Firstly they undergo secondary reactions either by collisions or spontaneously. They are then converted into either stable molecules, some of which may be different chemically from those originally present, or chemically unstable species (free radicals).

2.2 Production of ionizing particles

2.2.1 X- and gamma-rays

Neglecting the elastic scattering, these photons may interact with the atom (molecular binding is ordinarily unimportant) in one of three ways; photoelectric absorption, in which the photon disappears and single energetic electron is ejected; Compton scattering, in which the energy of the initial photon is shared between two products, a recoil photon and an ejected electron; pair production in which a pair of oppositely charged electrons appear. The probabilities of these three types of events depend upon the photon energy and upon the atomic number Z of the interacting atom.

2.2.2 Neutrons

The neutron is a nuclear particle, and we shall consider that it interacts with the nuclei only since the interactions between neutrons and electrons are exceedingly small. The main processes of neutron interactions with the nucleus are as follows:

Elastic scattering in which the neutron is scattered and loses energy which appears as kinetic energy of the recoil nucleus. The sum of the energies of all particles in the system remains constant.

Inelastic scattering, refers to $(n, n\gamma)$ reactions (e.g., $C^{12} (n, n\gamma) C^{12}$) in which the neutron is absorbed and re-emitted with loss of energy, leaving the nucleus in an excited state. The nucleus then decays to the ground state by emission of one or more gamma-rays

Capture processes considered here are the $H^1 (n, \gamma) H^2$ and $N^{14} (n, p) C^{14}$ reactions, in which the neutron is captured by the target nucleus forming a compound nucleus which may be excited and emits gamma radiation.

Non-elastic scattering, refers to reactions which result in the emission of particles other than a single neutron from the compound nucleus (e.g., $O^{16} (n, \alpha) C^{13}$).

At high enough energies, either two neutrons or other combinations of particles may be emitted. This is called spallation. For neutrons of energy greater than about 20 MeV, spallation reactions can be significant. In this case, the reaction products are generally several, and the local energy impartation is high. In our case, the cross section for this reaction is insignificant and

will be neglected. Non-elastic scattering begins at neutron energies of about 5 MeV, and becomes unimportant at an energy of about 10 MeV. For higher neutron energies, non-elastic scattering and spallation reactions become increasingly important and elastic scattering, which has a great importance at 15 MeV, is of less importance for energies greater than 20 MeV.

2.3 Energy deposition by directly ionizing particles

A moving charged particle exerts a transient electric force on the electrons in molecules which lie in the vicinity of its path. This impulsive electric field induces quantum transitions* in many of the molecules; thus energy is transferred to them causing the particle gradually to slow down.

A quantity of great value in the treatment of the absorption of charged particle by matter is the stopping power $S(E)$, defined as the energy lost by the particle per unit path in the substance. It is given by the equation

$$S(E) = - dE/dX$$

* Quantum mechanics states that atoms or molecules can exist only in a state which corresponds to one of the allowed states. Transitions between states may be induced by absorption of energy which enables the system configuration to pass over the energy barrier separating the two states. Such transitions may be the mutations common in genes.

where E is the classical kinetic energy. The stopping power varies with the energy of the particle and generally can be written as:

$$S(E) = - dE/dX = -(dE/dX)_{\text{collisions}} \\ - (dE/dX)_{\text{ionization}} - (dE/dX)_{\text{radiation}}$$

The penetration of electrons and positrons through matter is similar in many respects to that of heavy particles, for the basic interactions are the same. But there are important quantitative and even qualitative differences which come from the small mass of electrons, and from the fact that they commonly possess very great velocities. In addition to the two modes of energy loss for heavy particles (nuclear collisions and ionization), for electrons there is a third one, radiation loss, which occurs when an electron passes through the electric field of a nucleus where it loses energy by radiation. This energy appears as a continuous X-ray spectrum called bremsstrahlung or braking-radiation.

The energy loss per unit length because of radiation may be denoted by $(dE/dX)_{\text{rad}}$ as distinct from $(dE/dX)_{\text{col}}$ the energy loss by collisions (or ionization). The ratio of the two losses is given approximately by $(dE/dX)_{\text{rad}} / (dE/dX)_{\text{col}}$ equal to $EZ/800$ (Kaplan 1963),

where E is the energy of electron in MeV and Z is the atomic number of the absorber.

2.4 Macroscopic treatment of radiation absorption

Most of the experiments in radiation biology involve macroscopic problems. The macroscopic penetration problem is a vast one and its difficulties are legion. It is also fascinating, involving intricate interplay of transport, transformation, and transfer of energy.

The penetration of any variety of ionizing radiation into matter takes place by a very great number of sequential elementary processes that we have already discussed.

An important objective of radiation research is a complete description of the nature of the radiation present at any point in a medium as a function of the location of the point and the properties of the medium and of the radiation source. So radiation theory must be able to calculate this description (specification at each point in space of the types of radiation present there, and the intensities of each as a function of energy and direction of motion). Therefore, one energy parameter and a number of spatial coordinates are usually required; (the precise number depends on the geometrical arrangements of source and medium) on the basis of the probabilities (cross sections) of all relevant elementary processes.

CHAPTER III

ABSORBED DOSE OF NEUTRONS

Quantitative information on ionizing radiation can be furnished by certain quantities of classical physics (such as intensity or flux density) that have been available for many years.

However, for purposes of medicine, radiobiology, and radiation protection, the radiobiological physicist has found it necessary to develop other concepts which tend to characterize ionizing radiation in terms of its potential or actual interaction with matter. Historically speaking, such radiobiological quantities have been based on biological effects (e.g., erythema dose), on chemical effects (e.g., the pastille dose) or on physical effects (e.g., the absorbed dose). With one or two minor exceptions, modern quantities are all based on physical parameters.

3.1 Concepts and units of radiation dosimetry.

The International Commission on Radiological Units (ICRU) decided to initiate a thorough study of the quantities used in both "pure" radiation physics and in radiobiological physics in an effort to eliminate all ambiguities and to provide a coherent system of quantities and units for characterizing ionizing radiation in terms of its potential or actual interaction with matter.

A clear distinction should be made between the radiation to which an object is exposed to and the energy absorbed from this radiation. The quantity exposure (X) is defined as the

quotient of ΔQ by Δm , where ΔQ is the sum of all the electrical charges on all ions of one sign produced in air when all the electrons (negatrons and positrons) liberated by photons in a volume element of air whose mass is Δm , are completely stopped in air (ICRU 1964).

$$X = \Delta Q / \Delta m$$

The special unit of exposure is the roentgen (R).

$$1R = 2.58 \times 10^{-4} \text{ coulombs/kg.}$$

In measuring the exposure the quotient of energy by mass must be taken in an elementary volume in the medium which on the one hand is so small that a further reduction in its size would not appreciably change the measured value of the quotient energy by mass and on the other hand is still large enough to contain many interactions and be traversed by many particles. If it is impossible to find a mass such that both these conditions are met, the exposure can not be established directly in a single measurement, but multiple measurements that involve averaging procedure are required. Similar considerations apply to some of the other concepts defined.

The energy imparted by ionizing radiation to the matter in a volume is defined as the difference between

the sum of the energies of all the directly and indirectly ionizing particles which have entered the volume and the sum of the energies of all those which have left it, minus the energy equivalent of any increase in rest mass that took place in nuclear or elementary reactions within the volume. It should also be noted that most of the energy imparted will be degraded and appear as heat. Some of it, however, may appear as a change in interatomic bond energies. Moreover, during the degradation process the energy will diffuse and the distribution of heat produced may be different from the distribution of the imparted energy. For these reasons the energy imparted can not always be equated with the heat produced.

The absorbed dose is the quotient of ΔE_D divided by Δm , where ΔE_D is the energy imparted to the matter in a volume element, Δm being the mass of the matter in that volume element.

$$D = \Delta E_D / \Delta m$$

The absorbed dose depends on the nature and intensity of the incident radiation and on the nature of absorbing material. The special unit of absorbed dose is the rad (ICRU 1956).

$$1 \text{ rad} = 100 \text{ erg/g} = 1/100 \text{ joule/kg.}$$

The average energy (W) expended in a gas per ion pair formed is the quotient of E by N_W , where N_W is the average number of ion pairs formed when a charged particle of initial energy E is completely stopped by the gas (ICRU 1962).

$$W = E/N_W$$

The ions arising from the absorption of bremsstrahlung emitted by the charged particles are not to be counted in N_W . For air,

$$W(\text{air}) = 34 \pm 0.15 \text{ eV/ion pair} \quad (\text{ICRU 1962}).$$

The absorbed dose at a point in air (at NTP) that is surrounded on all sides by such material to a thickness at least equal to the range of secondary electrons and uniformly exposed to 1 roentgen of X- or gamma radiation is equal to

$$\begin{aligned} & (1 \text{ esu}/0.001293 \text{ g air}) \times (2.082 \times 10^9 \text{ electrons/esu}) \\ & \times (34 \text{ eV/ion pair}) \times (1.602 \times 10^{-12} \text{ erg/eV}) \\ & \times (1 \text{ rad}/(100 \text{ ergs/g})) = 0.87 \text{ rad} \end{aligned}$$

for all qualities of X- or gamma radiation with quantum energies greater than 20 keV, the energy range over which W is assumed constant. D_{air} will be referred to as the absorbed dose at point in an extended mass of air under

equilibrium conditions.

If any ionization chamber or other measuring instrument has been calibrated in roentgens, records an exposure X, then the absorbed dose is given by

$$D_{\text{air}} = 0.87 \times X \quad \text{rad.}$$

If the exposure dose at any point in the irradiated medium is X roentgens, then the absorbed dose in tissue or other material exposed to X- or gamma radiation in the medium at the same point is given by

$$\begin{aligned} D_{\text{medium}} &= D_{\text{air}} \times (\mu_{\text{en}})_{\text{medium}} / (\mu_{\text{en}})_{\text{air}} \\ &= 0.87 X \times (\mu_{\text{en}})_{\text{medium}} / (\mu_{\text{en}})_{\text{air}} \\ &= f(X) \text{ rad} \end{aligned}$$

where (μ_{en}) is defined as the energy absorption coefficient (in cm^2/g) of the medium or of air, to be evaluated for the total spectrum of X- or gamma radiation arriving at the point of interest, and f is the absorbed dose in rads per roentgen of exposure dose.

The values of the mass energy absorption coefficient for a number of elements and for water, air, bone and muscle have been tabulated by Rosemary T. Berger (1961). These tables also contain values of f in water, muscle, and bone for monochromatic photon energies.

Mean values, \bar{f} , of f are integrated over several typical primary X-ray spectra (ICRU 1956).

In the case of neutrons only the first collisions have to be taken into account if the thickness of the medium under consideration is appreciably smaller than the mean free path of neutrons in the medium. In order to describe clearly and quantitatively this transfer of energy from indirectly ionizing particles to directly ionizing particles in an irradiated material, the new quantity kerma (kinetic energy released in material) has been introduced. The kerma (K) is defined a quotient of ΔE_k by Δm , where ΔE_k is the sum of the initial kinetic energies of all the charged particles liberated by indirectly ionizing particles in a volume element (ICRU 1964).

$$K = \Delta E_k / \Delta m$$

It should be also noted that since ΔE_k is the sum of the initial kinetic energies of the charged particles liberated by indirectly ionizing particles, it includes not only the kinetic energy of these charged particles but also the energy they radiate in bremsstrahlung. The energy of any charged particles is also included when these are produced in secondary processes occurring within the volume element. Thus the energy of Auger elec-

trons is part of ΔE_k .

It is also helpful to note that a fundamental physical description of a radiation field is the intensity (energy flux density) at all relevant points. For the purpose of dosimetry, however, it is convenient to describe the field of indirectly ionizing particles in terms of kerma rate ($\Delta K/\Delta t$) for a specified material. A suitable material would be air for electromagnetic radiation of moderate energies, tissue for all radiations in biology and medicine, or any relevant material for studies of radiation effects. When charged particle equilibrium exists at some point in a material of interest, the kerma is equal to the absorbed dose if bremsstrahlung losses are negligible. In beams of X- or gamma-rays or neutrons whose energies are moderately high, transient charged particle equilibrium can occur. In this consideration the kerma is slightly less than the absorbed dose. At very high energies the difference becomes appreciable. In general, if the range of directly ionizing particles becomes comparable with the mean free path of the indirectly ionizing particles, no equilibrium will exist.

The degree of biological damage produced by ionizing radiation depends not only on the amount of energy absorbed but also on the spatial distribution of the

energy deposition on a microscopic scale. Since the energy is transferred to atoms and molecules situated in or near the tracks of charged particles, it has been considered convenient to express the heterogeneity of energy deposition in terms of the linear density of energy loss in these tracks. For this purpose we introduce the term linear energy transfer (LET). It will be clear that the interpretation of the term "locally absorbed energy" in the definition of LET as "the linear rate of energy loss (locally absorbed) by an ionization particle traversing a medium" may be rather difficult. Various cut-off levels of energy have been selected to separate δ -ray (knock-on electron) tracks from the track of the primary particle (Report of the RBE Committee to the ICRP and ICRU). It has been recommended that the cut-off level should be indicated by a subscript, e.g. LET_{100} , would indicate an LET obtained when tracks due to secondary particles with energies above 100 eV are counted as separate tracks. The simplest parameter is the LET_{∞} , called total particle LET and defined as the energy loss per unit distance travelled by the primary particle, thus being equal to the stopping power. A particle of unit charge moving at a velocity corresponding to minimum specific ionization, imparts the minimum LET of approximately 0,19 keV/ μ of

water. If the charge is greater and the velocity is lower, the LET can reach values of many hundred keV per micron.

The objective of the dosimetry of neutrons and other heavy charged particles must be usually more than a mere determination of the absorbed dose. The relative biological effectiveness (RBE) is used to compare the effectiveness of absorbed dose of radiation delivered in different ways, has been represented by the symbol γ . The statement that "the RBE of alpha radiation is 10" signifies that γ rads of alpha radiation produce a particular biological response in the same degree as 10 γ rads of gamma radiation. The concept of RBE has a limited usefulness because the biological effectiveness of any radiation depends on many factors. Thus the RBE of two radiations cannot in general be expressed by a single factor but varies with many subsidiary factors such as the type and degree of biological damage (and hence with absorbed dose), the absorbed dose rate, the fractionation, the oxygen tension and the temperature

Thus analysis for the purpose of either radiobiology or radiation protection of irradiation by neutrons or heavy charged particles must include information which is related to the LET of the charged particles that deliver the absorbed dose, and the information which is related

to RBE to compare the effectiveness of absorbed dose delivered in different ways.

3.2 Interaction between neutrons and tissue

Determination of absorbed dose in tissue exposed to fast neutron radiation on the basis fluence involves more elaborate calculations. First of all the interactions that occur between neutrons and tissue depend upon the composition of the tissue material been used. The atomic composition of the tissue material should be taken into consideration to evaluate the more probable interactions of neutrons and the atoms of the tissue.

For fast neutrons, the most important interactions between neutrons and tissue is elastic scattering. When a neutron strikes a proton (another billiard ball of same mass) anything up to the whole of the neutron energy can be transferred to the proton. On the other hand, when it collides with a much heavier nucleus it rebounds without losing very much energy. It has been estimated that between 70 - 95 % of the energy absorption takes place via recoil protons (Randolph 1957).

The other major contribution to the absorbed dose in tissue is by inelastic nuclear reactions and asymmetric distribution of recoils from elastic scattering with C, N, and O. These inelastic reactions contribute of 5 - 30 % to

the total dose. The relative contribution to the absorbed dose from these sources and from elastic collisions with C, N, and O are summarized in figure 1. The contribution of slow neutrons to the absorbed dose is not likely to be very important. Slow neutrons are absorbed in tissue mainly by the (n,γ) reaction in hydrogen and the (n,p) reaction in nitrogen.

The energy deposition in hydrogenous materials by 14.1 MeV neutrons was calculated by Randolph (1957) by assuming the contribution of inelastic scattering and the asymmetric distribution of recoils from elastic scattering to the absorbed dose (see table I).

Table I

Energy deposition in hydrogenous materials
by 14.1 MeV neutrons.

	Percent of dose by component elements				Percent of dose by nuclear processes		
	H	O	N	C	H Elas.	C,O,N,Other Elas. Inelas.	
Standard man	69.5	6.5	1.1	22.0	69.5	4.3	26.1
Tissue approxi- mation	69.5	5.4	1.2	24.0	69.5	4.2	26.4

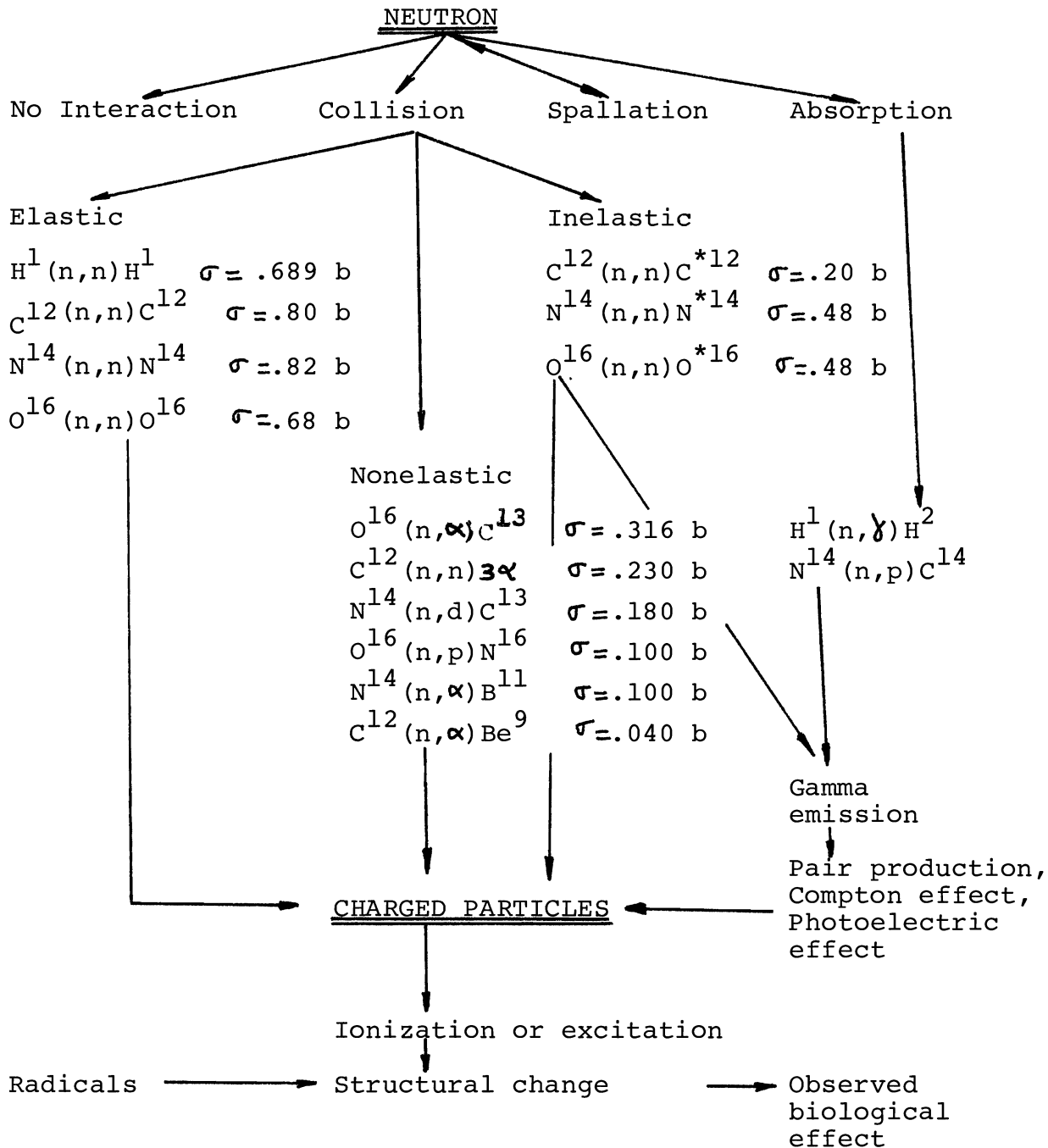


Figure 1. Schematic diagram to illustrate the interaction of fast neutrons with tissue.

3.3 Method of dosimetry.

3.3.1 General.

One of the most important aspects of experimental nuclear physics is the problem of detection, identification, and energy determination of radiations emitted in nuclear reaction and decay. All methods of detection of ionizing radiations depend on their interaction with the matter that they traverse. This interaction, as was explained previously, produces ionization, or excitation of the extranuclear electrons, and the operation of different detectors depends on the resultant effect of one of these processes.

Ionization chambers are one of the most common instruments for determination of radiation dose. The essential parts of the ionization chamber are two electrodes kept at different potentials and a gas that fills the space between two electrodes. The measuring instrument (electrometer) is attached to the collecting electrode. The collecting electrode is ordinarily, but not necessarily, at a potential close to ground potential. The other electrode, which is ordinarily kept at a constant voltage V_0 of several hundred to several thousand volts to provide a field for ion collection, is called the high voltage electrode. The collecting electrode is supported through insulators by another electrode which is held at constant voltage, approximately equal to that of the collecting electrode itself. This is called a guard electrode. The guard electrode is connected through insulators to the high voltage electrode. The purpose of the guard

electrode is to prevent leakage currents from reaching the collecting electrode and to prevent irregularities of the electric field near the edges of the collecting electrode.

3.3.2 Tissue-equivalent chambers.

The measurement of the ionization in the gases may be considered to be a direct and sensitive method for determining the energy deposited in biological material. The absorbed dose may be obtained by applying the relation between the ionization produced in a gas-filled cavity at the place of interest in the material irradiated, and the energy imparted to unit mass of the material. If the cavity is sufficiently small, the gas will be exposed to the same flow of ionizing particles as the material under consideration. The absorbed dose D , in ergs per gram of material, is then related to the number of ion pairs formed per gram of gas, J , by the equation:

$$D = J W s,$$

where W is the average energy in ergs expended per ion pair by the ionizing particles crossing the cavity, and s is the effective value of the ratio of the mass stopping power of the medium to that of the cavity gas for these ionizing particles. The above equation known as the Bragg-Gray relation, may only be applied if the following requirements are satisfied;

1. The introduction of the gas-filled cavity must have a negligible effect on the distribution of the charged particles in the medium, which implies that the linear dimensions of the cavity must be small in comparison with the ranges of these particles in the cavity.

2. The intensity of the primary radiation must be

substantially constant in the cavity and the surrounding wall.

3. The solid medium surrounding the cavity must be of such a thickness that charged particle equilibrium is achieved. In this way all the particles crossing the cavity originate in the medium.

In the case of fast neutron irradiation in tissue only the case where corpuscular equilibrium conditions for the recoil protons exist will be considered here because the proton ranges are generally very small, and hence equilibrium will exist in most cases.

Some of these requirements are eliminated or much more easily fulfilled if both wall and gas are of equal atomic composition. In this case s will be equal to 1, so that the absorbed dose is given by the relation

$$D = J' W,$$

where J' is the number of ion pairs formed per gram of the wall-equivalent gas. The Bragg-Gray relationship can generally be used for any ionization chamber and various types of radiations (Gray 1937).

3.3.3 Relative contribution of gas and wall of the chamber

Most types of ionization chambers contain a permanent gas filling. However, owing to changes in the gas composition the sensitivity of the tissue-equivalent chamber may alter. This change in sensitivity is caused

by the absorption and diffusion of the gases in the tissue-equivalent material. The ionization current measured in a tissue-equivalent chamber is produced through recoil protons and heavier nuclei released by the incident neutron beam. The relative contributions of recoil particles released from the wall and from the contained gas, respectively, depend on the ratio of the ranges of these particles and the dimension of the chambers. Since recoil protons deliver the largest contribution to the total dose, only these protons will be considered. For the 14 MeV neutrons, the ranges of mean energy protons resulting from elastic collisions are equal to about 70 cm, for a tissue-equivalent gas mixture consisting of methane, carbon dioxide and nitrogen at normal temperature and pressure. These ranges exceed the chamber dimensions by a factor of at least 30. So the ionization of the gas will be largely produced by protons released from the wall of the chamber.

With carbon dioxide as the filling gas of the chamber in the low pressure region, the response of the chamber will be proportional to the pressure. At rather high pressure, the protons from the wall can be completely stopped in the gas, the proportionality will no longer exist. With methane as the filling gas, the ionization will be partly produced by protons generated in the wall of the chamber and partly by protons which originate in the gas

itself. For low pressures the ionization current increases proportionally with the pressure as long as the range of the recoil protons exceeds the chamber dimensions sufficiently, i.e., as long as the wall effect predominates (Abersold and Anslow 1946, Anglinzew 1961). The contribution of the gas becomes important at higher methane pressures; part of the current will be proportional to the square of the pressure since the number of recoil protons, and the number of ionizations produced by these protons both increase proportionally with the pressure. The protons will deliver all their energy in the chamber if the ranges of the recoil protons are smaller than the chamber dimensions.

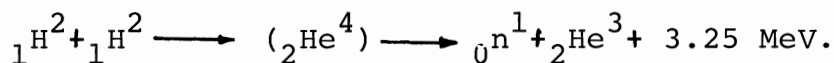
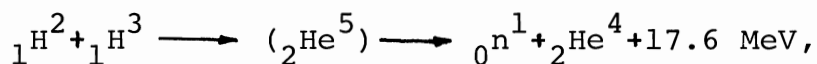
It may be concluded that for 14 MeV neutron irradiations the recoil protons which ionize the gas in the chamber originate mainly in the wall of the chamber, and therefore, small variations in the gas composition will not change the measured neutron dose.

CHAPTER IV

OPERATION AND YIELD OF NEUTRON GENERATOR

4.1 Nuclear reactions of neutron generator.

The neutron generator is designed to produce high current beams of protons and deuterons incident upon targets loaded with either deuterium or tritium. Fast neutrons are produced by the reactions



These two reactions are frequently written in the shorthand notation, (D,T) and (D,D).

Fast neutrons of 14.1 MeV and 2.6 MeV are produced by the reactions (D,T) and (D,D) respectively. For deuteron bombarding energies up to 150 keV, the differential yield of the neutrons from (D,T) reaction is nearly isotropic, that is, the number of neutrons/steradian is nearly the same. For the purpose of this work, thin targets are used since it is desirable to minimize the energy spread of the incident particles.

4.2 Operation and design of the neutron generator

Operation of the Texas Nuclear neutron generator depends on production, extraction and acceleration of ions. After acceleration, the ions are allowed to fall on a suitable target material to produce neutrons. Positive

ions produced in a radio-frequency type ion source are extracted by applying a potential across the ion source bottle. After extraction, the ions are focused by a gap lens situated directly below the exit canal of the ion source bottle. After leaving the gap lens, the ions enter the field of the accelerating tube where they are accelerated through a potential of 300 KV and distributed between 20 electrodes which are separated equally by adjacent insulators. An ion passing through the accelerating tube experiences a "kick" of 15 KV (300 KV divided by 20 electrodes) to have smooth multistage acceleration. Electrostatic lines of force between the gap lens and the first electrode, and between adjacent electrodes, tend to restrict the beam to the center of the tube and thus aid in focusing. The shape and spacing of the electrodes are very critical in determining the focal properties of the accelerating tube. After leaving the accelerating tube, the ions drift through a potential free region (drift tube) until they fall on the target.

4.2.1 Ion source and gap lens

The ion source consists of a pyrex bottle, a palladium leak, an r-f oscillator, a solenoid which fits around the pyrex bottle, an extraction power supply, power supply for the lens, solenoid and oscillator, and a quartz sleeve

which fits around the exit canal.

A controllable flow of deuterium or hydrogen gas to the ion source bottle is maintained by using a palladium leak. The ion source bottle is part of the main vacuum system and the flow of gas out of the ion source bottle into the main vacuum system is restricted by small size of the exit canal. A radio-frequency (r-f) field applied to two excitor rings causes intense ionization of the deuterium gas (or hydrogen) gas. The positive ions in the discharge are focused towards the exit canal by applying a positive potential across the bottle. A solenoid coil, which fits around the bottle and seats on the ion source base, produces a magnetic field with lines of force are in the direction of the long axis of the bottle. The magnetic field produced by the solenoid restricts the particle paths to the center portion of the bottle and causes them to spiral towards the exit canal. The pyrex shield directly below the extractor probe protects the probe from particle bombardment. The quartz sleeve which surrounds the aluminum exit canal serves to hide the metal canal from discharge thus preventing surface recombination of the ions. The ions leave the canal in all directions, and hence, must be focused before entering the accelerating tube. This is the function of the gap

lens. A schematic drawing of the gap lens is shown in figure 2.

Available potential 0-10 KV (negative with respect to the ion source base plate) is applied to the gap lens to determine the focal length of the ion beam. After the beam leaves the gap lens it enters the accelerating tube.

4.2.2 Accelerating tube

This tube is designed for multi-stage acceleration and consists of 20 electrodes which are separated by insulators. A schematic drawing of the gap lens and first few sections of the accelerator tube is presented in figure 3.

The first electrode is connected to the ion source base, so it is at a positive potential with respect to the gap lens. The field lines between this electrode and the gap lens have a focusing effect on the beam. The second electrode is negative with respect to the first, the third is negative with respect to the second, etc., so the lines of force between successive electrodes tend to restrict the beam towards the center position of the tube. The high voltage (300 KV) is divided equally down the tube so that the beam receives a kick of 15 KV in passing each electrode.

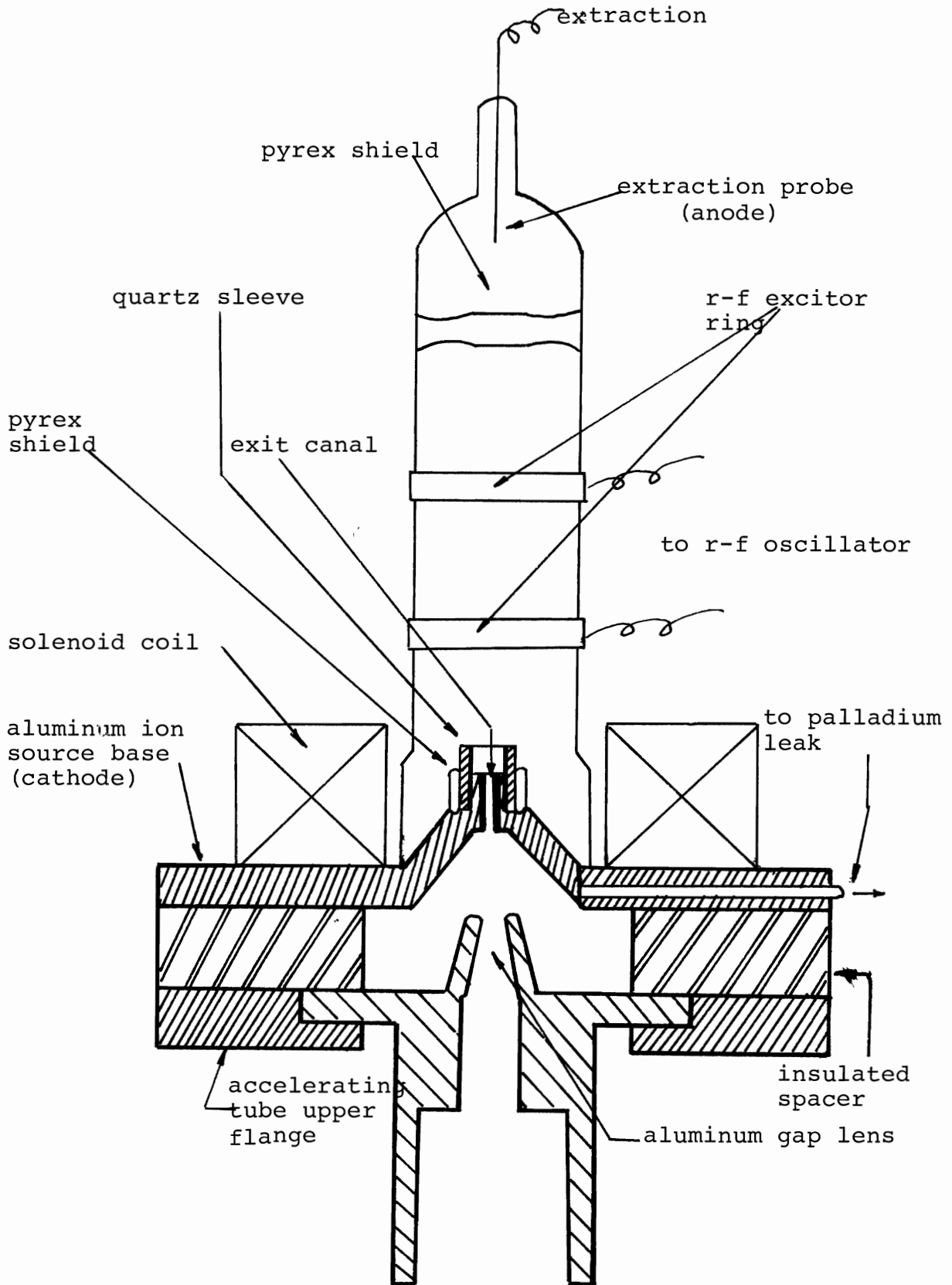


Figure 2. Schematic of ion source and gap lens.

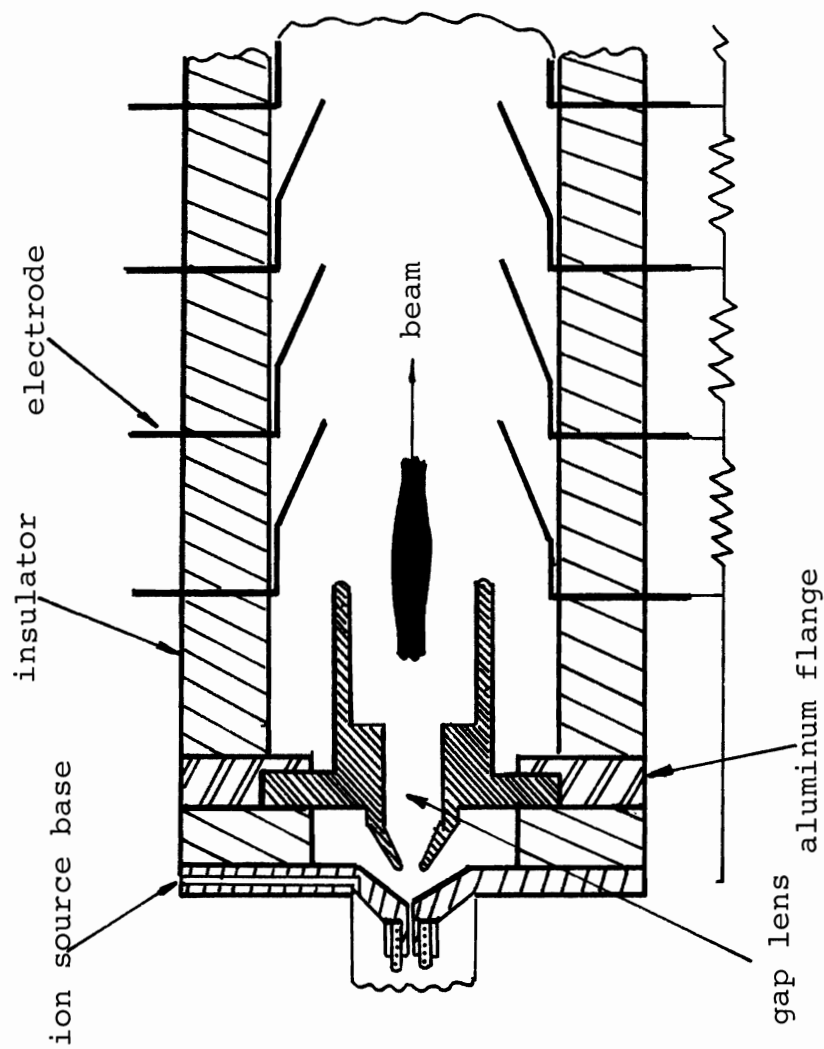


Figure 3. Accelerating tube and gap lens. The electrodes are designed to shield insulators from stray beam and "back streaming electrons."

4.2.3 Drift tube and target assembly

The beam emerging from the accelerating tube is moving at a high velocity and it continues at this velocity through the potential free drift tube section of the machine until it is stopped at the target. The so-called drift tube section is at ground potential and is attached to the accelerator tube at the center base plate of the machine. Drift tube consists of the following components:

- 1- A T-section of stainless steel tubing which connects the base plate to the diffusion pump.
- 2- A section which contains a thermocouple vacuum gauge and a pump out valve.
- 3- A beam catcher and viewer assembly.
- 4- A set of adjustable deflector plates.
- 5- A target bellows.
- 6- The target assembly.

The thermocouple vacuum gauge measures the pressure in the system when the vacuum is relatively poor. When targets or other components in the vacuum system are to be changed, the system is brought to atmospheric pressure by introducing dry air (or dry nitrogen) through the pump out valve.

In order to localize the area where the beam strikes,

a beam catcher is placed immediately after the deflector plate. The catcher is a threaded rod which can be moved in and out without disturbing the vacuum. Before allowing the beam to fall on the target, it is sometimes desirable to know the location and size of the beam spot. For this purpose, a beam viewer is situated directly across from the beam catcher.

The target assembly of the neutron generator consists of a target holder, a water jacket, and an electron suppressing electrode (see figure 4). The target is cooled by approximately 0.2 gallons of water per minute through the water gap. The electron suppressor is isolated from the target cap and the bellows by glass insulators. A negative potential of 90 volts is applied to the suppressor to force electrons which are ejected from the target during bombardment to return to the target.

4.3 Shielding of neutrons

The radiation resulting from operation of the neutron generator requires that the generator be properly shielded for safety. The main requirements to be considered in designing a shielding and collimating system are:

- 1- The need for minimum transmission of radiation outside the useful beam.

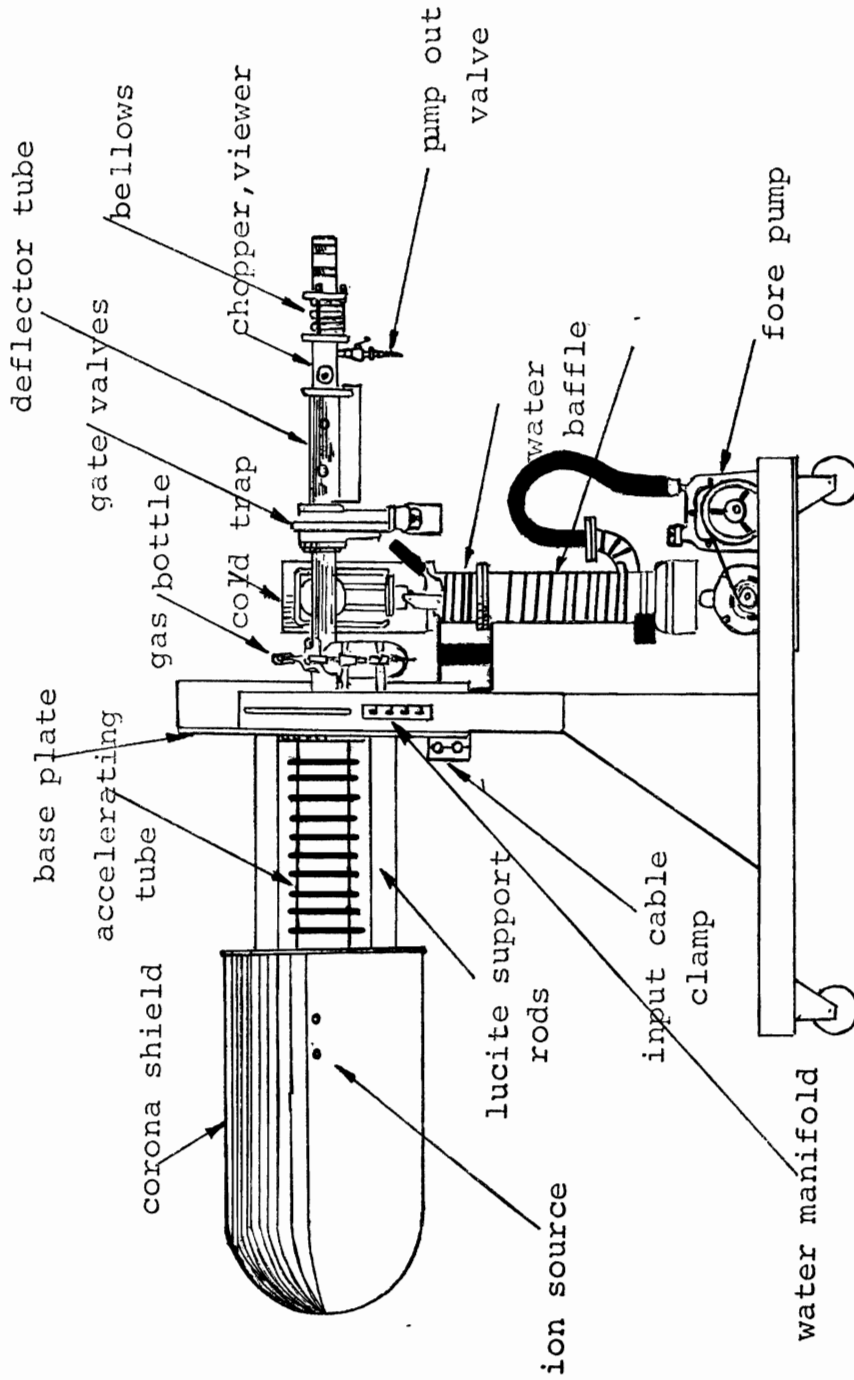


Figure 4. Outline drawing of the neutron generator.

- 2- The need to limit the size and weight of the system so that it can be made mobile to provide a steerable beam.
- 3- The loss of available output by inverse square law as the total thickness of the shield is increased.

Shielding for fast neutrons is a complex topic encompassing the entire field of neutron interactions. Most of the available information on shielding refers to specialized subject since there have been relatively few fundamental discussions published about it.

Since the biological damage induced by neutrons increases with increasing neutron energy, for 14 MeV neutrons, the maximum permissible dose for a 40 hour week is 10 neutrons/(cm²-sec) compared to 18 neutrons/(cm²-sec) for 1 MeV neutrons or 670 neutrons/(cm²-sec) for thermal neutrons. Furthermore the higher neutron energy, the more difficult it is to shield. For example, 30 cm of water will decrease the dose due to 1 MeV incident neutrons by a factor of approximately 100,000, whereas the same thickness of water reduces the dose due to 14 MeV incident neutrons by only a factor of about 10.

Shielding fast neutrons is usually accomplished by slowing down energetic neutrons to thermal or near thermal

energies and then capturing them. The most effective way to decrease the energy of the neutron is to require that it makes multiple elastic collisions with light nuclei. A hydrogenous material is the logical choice for shielding since the neutron will lose more energy per collision with hydrogen than with any other atom. After neutrons have been slowed down by collision with light nuclei they will usually be captured through a nuclear reaction. For this purpose boron and cadmium are two suitable elements. Another and more recent method for slowing down the neutrons is to utilize the high cross sections for elastic and inelastic collisions in steel or copper. The moderated flux is then allowed to interact with hydrogenous materials such as polyethylene or paraffin which can be more effective for these lower energy ranges. The $(n,2n)$ reaction is very important since it reduces the neutron energy 22-35 % per collision. For high neutron energies inelastic scattering becomes important in materials containing elements of higher atomic weight. For these reasons it is desirable that in fast neutron shields various components should be combined with heavier elements. For this purpose it is necessary that a neutron shield consists of an inner core of steel (as the heavier element)

which serves mainly to attenuate primary neutrons, a layer of hydrogenous material, which is less efficient than steel at stopping the primary neutrons, but is more efficient at stopping scattered neutrons (Greenland and Thomas 1969). Furthermore, a third component of the shield may be required for the effective capture of thermalized neutrons without emission of energetic gamma-rays. In this case thermalized neutrons are captured by boron or cadmium and lead layers can be used to stop gamma-rays from this capture process.

CHAPTER V

EXPERIMENTAL PROCEDURE, RESULTS, AND DISCUSSION

5.1 The tissue-equivalent ionization chamber

The tissue-equivalent ionization chamber was designed for the measurements of ionization produced by a fast neutron flux. The ionization chamber which has a length of 14.10 cm and an external diameter of 2.42 cm, is shown in figure 5. For obtaining charged particle equilibrium the walls of the chamber were made 0.86 cm thick for neutrons of 14.1 MeV. A guard ring was used to make it possible to measure accurately the ionization currents at low dose rates. The central electrode was also a tissue-equivalent rod of 0.40 cm in diameter.

The volume from which ions are collected was calculated from the dimensions to be 5.15 cm^3 to an accuracy of $\pm 0.002 \text{ cm}^3$. The percentage composition by weight of the materials which have been used was : 10.2 hydrogen, 76.2 carbon, 3.5 nitrogen, 5.2 oxygen, and 4.9 other elements (Shonka 1958). In order to eliminate some requirements and simplify the Bragg-Gray equation, the chamber was filled with a gas which had an atomic composition very close to that of walls of the chamber.

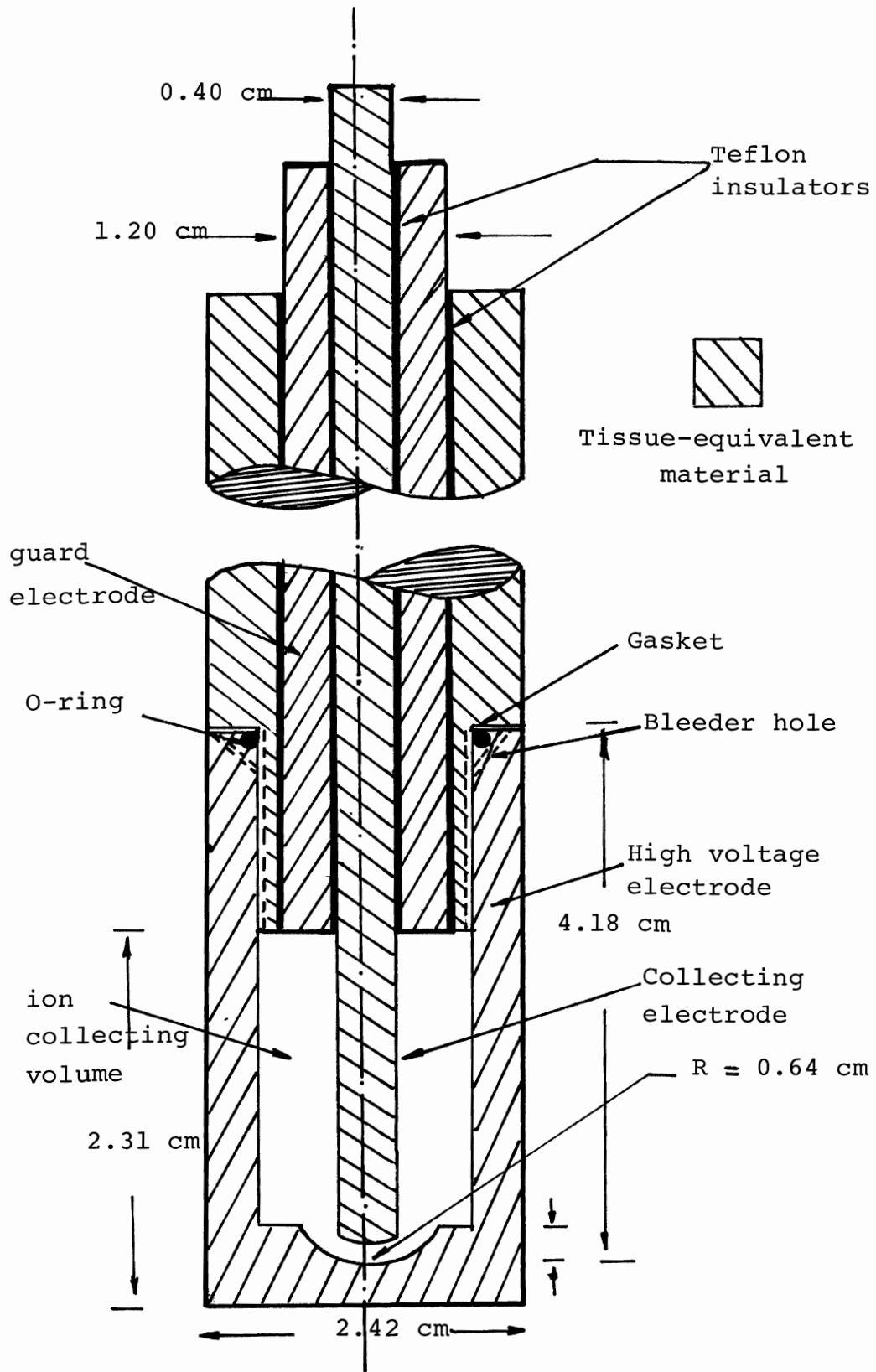


Figure 5. Schematic drawing of the tissue-equivalent ionization chamber used for dosimetry of neutrons.

The collecting electrode and the guard area around the electrode are held at ground potential while a positive collecting voltage is applied to the front plate. The applied voltage was 50 volts. Measurements showed that this was sufficient to permit collection of all ions (see figure 6).

The ion current was measured with a Keithley model 640 electrometer operating in "integrate mode". In this mode the current is permitted to charge a 20 picofarad \pm 0.25% guarded capacitor in the feedback loop, contained within the electrometer, to a voltage V, in a certain time. The charge collected during this time is then $2V \times 10^{-11}$ coulomb.

5.2 Shielding of the generator

In the experiments the attenuating characteristics of the following materials were examined either alone or in combination with each other:- paraffin, steel, borated paraffin, lead, water. Since there is no obvious optimum combination for relative or total thickness of these materials, several combinations were studied. General arrangement for attenuation experiments is shown in figure 7 . Flat slabs of paraffin and borated paraffin (thickness 20 cm) with an area 20 cm by 40 cm, slabs of paraffin (thickness 4 cm) with an area 30 cm by 40 cm

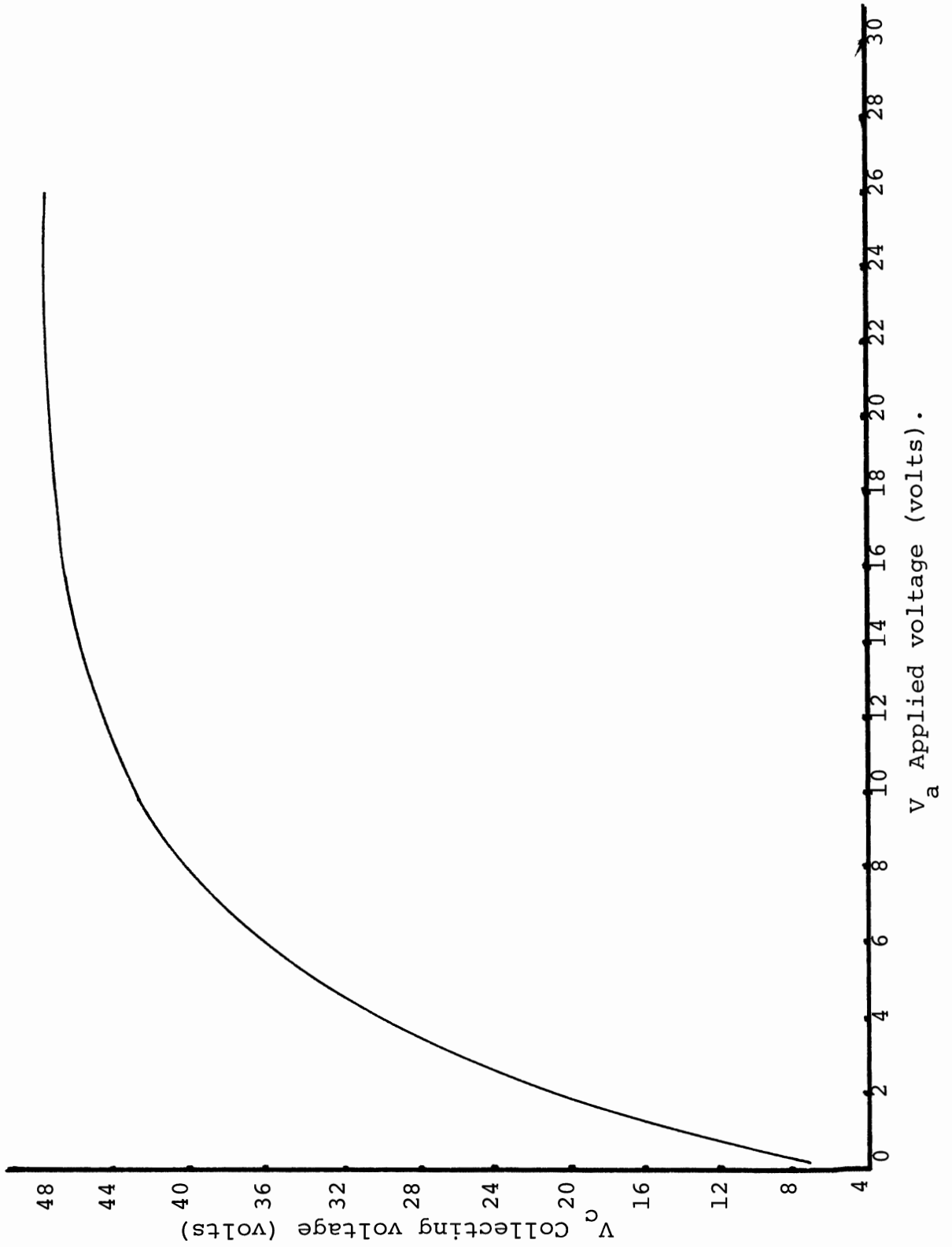


Figure 6. Saturation curve of the tissue-equivalent ionization chamber.

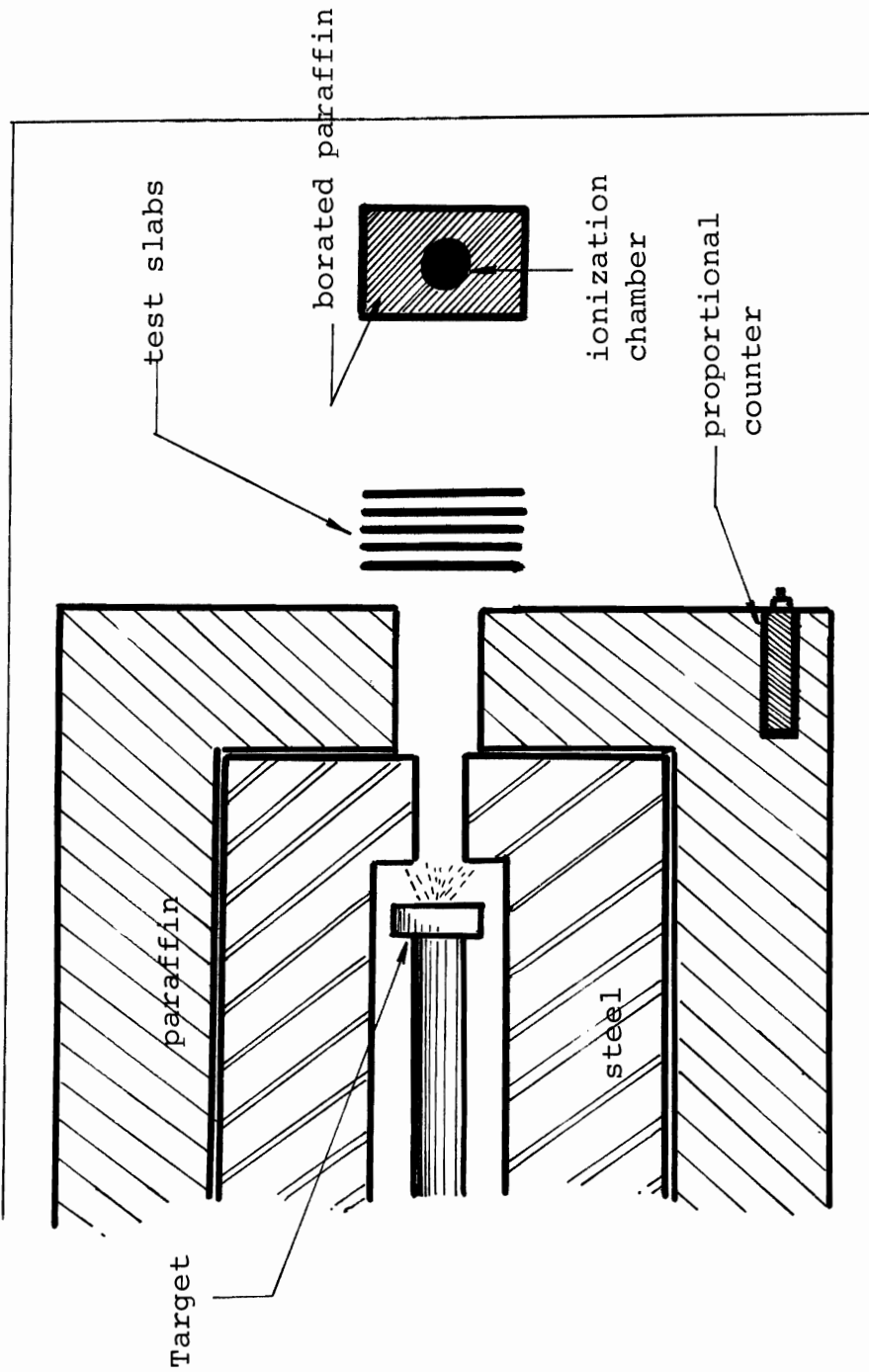


Figure 7. Generator shielding arrangements.

and steel blocks (thickness 5 cm) with an area 10 cm by 20 cm were used.

5.3 Experimental procedure

The neutron generator was operated at a voltage range from 80 KV to 120 KV and a deuteron beam current of 300-400 μ A. The detector was mounted in line with the accelerator tube of the neutron generator and after the first measurement of ionization current without any attenuator, the chamber was completely surrounded by borated paraffin blocks to prevent detection of scattered neutrons. The slabs were successively placed in the beam and in this way, the shielding thickness could be increased while the detector remained in the same position, consequently no inverse square law corrections were necessary.

Since the measurement of ionization in gases can be considered to be a direct and sensitive method for determining the energy deposited in biological material, the ionization current was determined at a distance of 60 cm from the target with and without shielding of the ionization chamber. The counting rate resulting from the proportional counter and the dose rate obtained with the ionization chamber were measured for each slab thickness. The ratio of the ionization current to the counting rate of the proportional counter was

recorded and found to vary less than 3 % for any particular set of absorbers.

Also in order to observe the contribution of gamma-rays produced from shielding materials to the ionization current, several materials were activated for a suitable time and their spectra were obtained and analysed by a multi-channel analyser (model TMC 400). The spectra of activated steel are presented in figures 8 and 9.

5.4 Determination of the absorbed dose

The absorbed dose in the tissue-equivalent chamber (at NTP) uniformly exposed to X equivalent roentgen of a given flux of fast neutrons is given by the relation

$$D = (X) (1 \text{ esu}/0.001293 \text{ g of gas}) (2.08 \times 10^9 \text{ electrons/esu}) \\ (34 \text{ eV/ion pair}) (1.602 \times 10^{-12} \text{ erg/eV}) (1 \text{ rad}/100 \text{ erg/g}) (s)$$

or absorbed dose will be equal to

$$D = (0.90) (X) (s) \text{ rad,}$$

where X ($\approx Q/\text{volume}$) , the equivalent roentgen, is the ratio of the total charge collected to the effective volume of the ionization chamber. The total charge Q ($\approx CV$) produced by ionizing radiation in the chamber and collected by the capacitor C (20 picofarad) which has been charged to voltage V (volts) (see section 3.1).

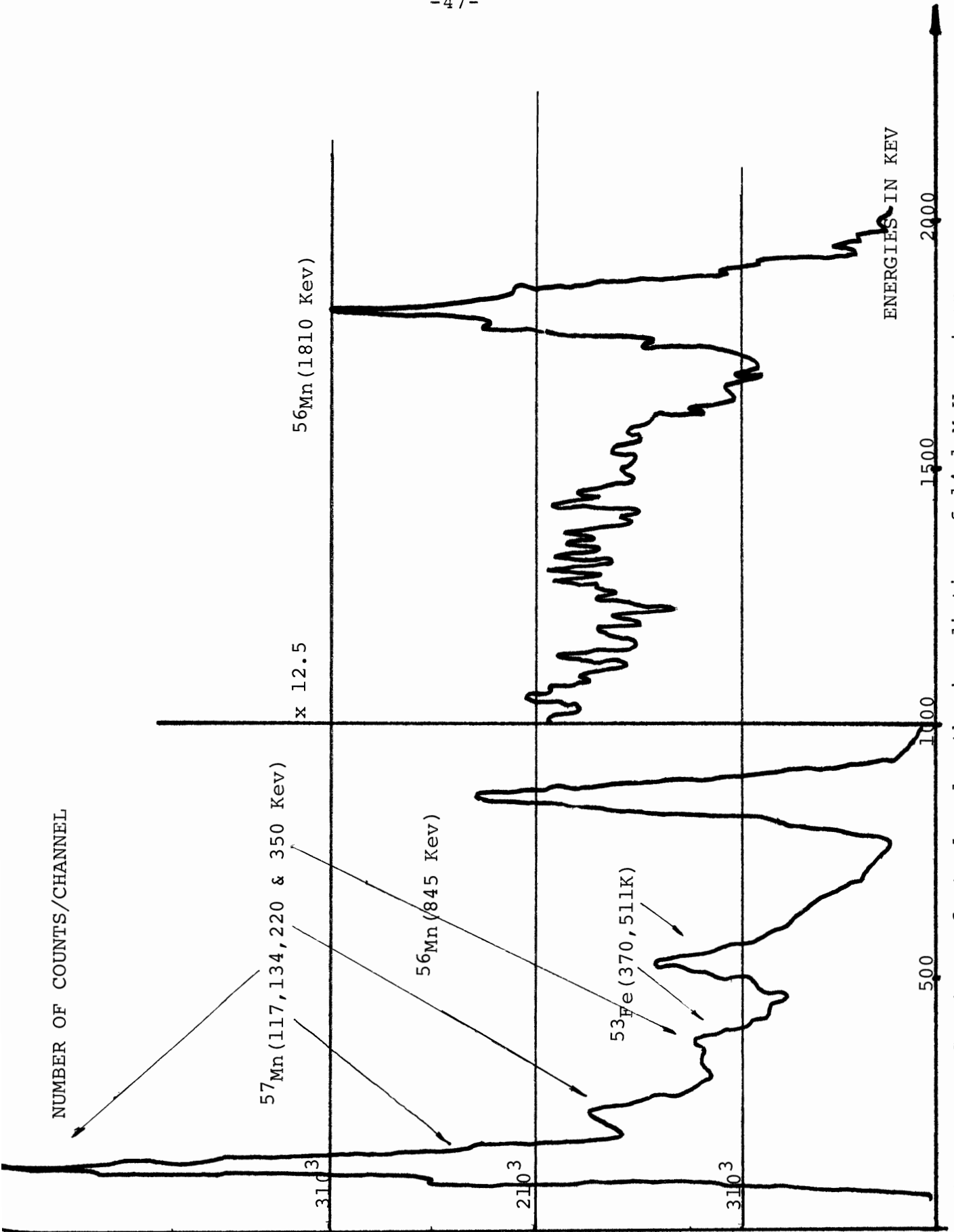


Figure 8. Spectrum of steel under the irradiation of 14.1 Mev neutrons.

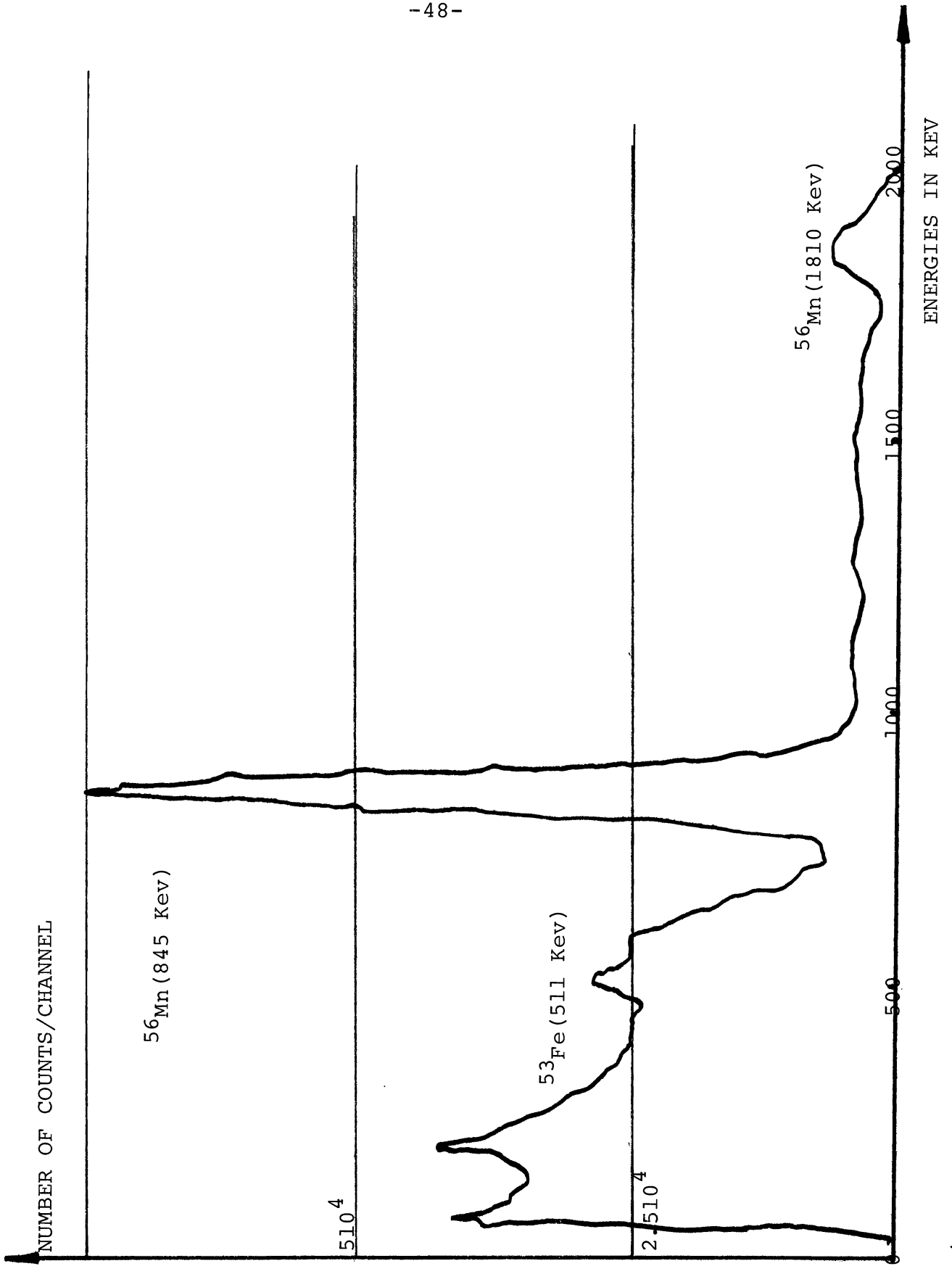


Figure 9. Spectrum of steel under the irradiation of 14.1 MeV neutrons.

It should be noted that the average energy W expended by ionizing particles crossing the cavity per ion pair formed was used as 34 eV for neutrons (ICRU 1956). s is the stopping power per unit mass of the protons generated by the neutron flux, or, strictly the weighted average stopping power for all recoils. Since both wall and gas are of the same atomic composition, s will be equal to 1 (see section 3.3.2). Then the absorbed dose becomes

$$D = (0.90) \times (Q(\text{esu})/\text{volume}(\text{cm}^3)) \text{ rad},$$

where $Q=CV$ and $\text{volume} = 5.15 \text{ cm}^3$

$$\text{or, } D = ((20 \times 10^{-12} \text{ farad})(3 \times 10^9)) / ((5.15 \text{ cm}^3)(0.90)) \text{ rad}$$
$$D = 10.48 \times (V \text{ volts}) \text{ rad}.$$

5.5 Attenuation results and discussion

In the experiments the ionization chamber was placed in the forward direction of the maximum flux density. The ionization current and the counting rate per minute by the proportional counter was registered for each slab thickness. The attenuation curves obtained are shown in figures 10, 11, and 12.

The experimental data for paraffin are shown in table II. Figure 10 shows the D_x/D_o (D_o and D_x are equal to the neutron dose rates measured without

Table II

Attenuation of 14.1 MeV neutrons by paraffin.

H.V = High voltage = 80 KV, I = Beam current = 400 μ A.

Ionization chamber was placed at a distance of 60 cm from the target.

Thickness of paraffin (cm)	Ionization current i (mV)	Proportional counter p (counts /min.)	i/p	Corrected ionization current i' (mV)	Dose rate D (rad /min.)	Transmission factor D_x/D_0
-	6800	32596	.209	6800	.714	1.00
4	7200	40828	.176	5699	.598	.84
8	6310	42344	.150	4857	.509	.71
12	5290	42056	.126	4080	.428	.60
16	4375	41377	.105	3400	.357	.50
20	3550	38495	.093	3008	.316	.44
24	2675	34334	.078	2519	.264	.37

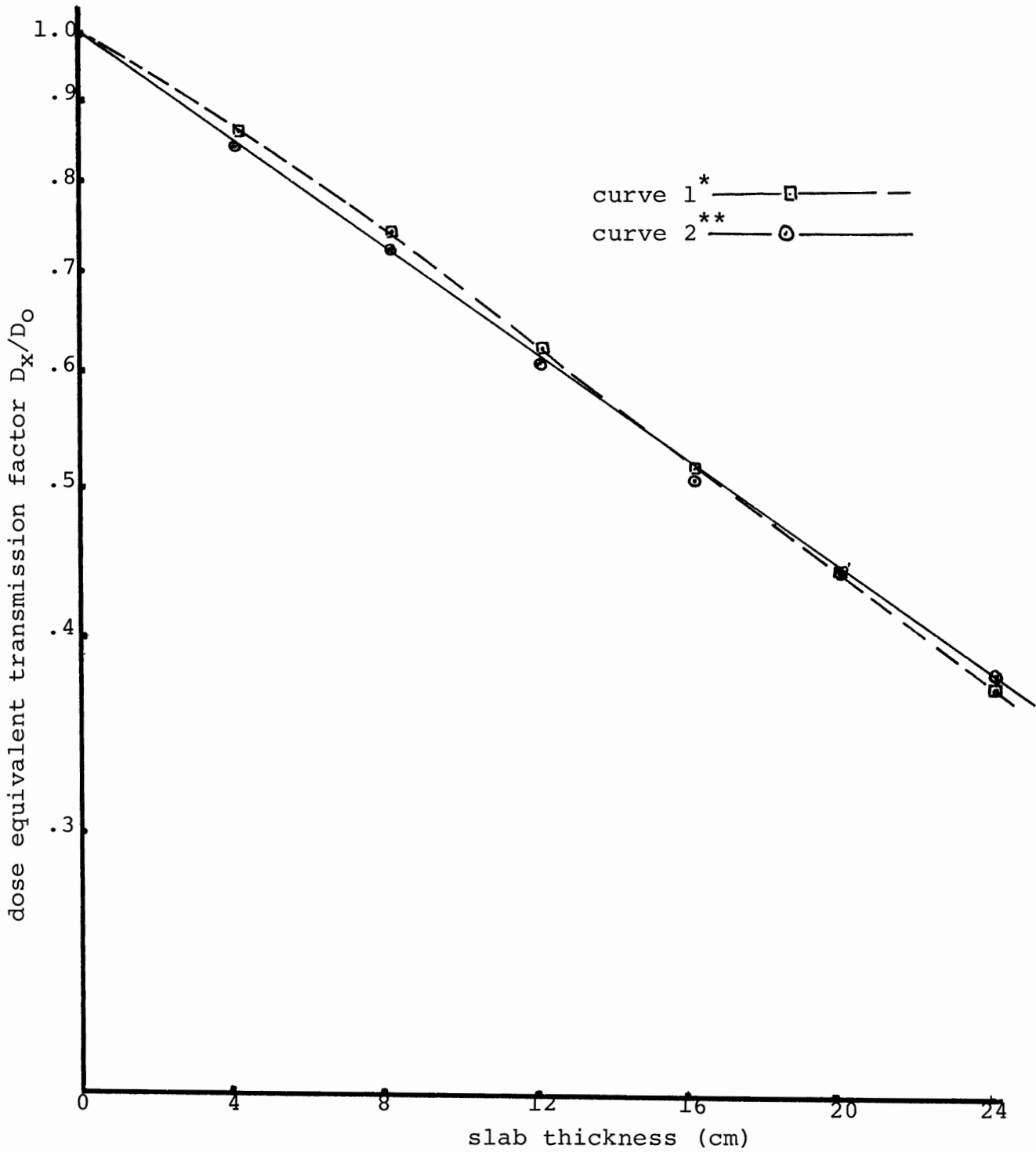


Figure 10. Relative dose equivalent values as a function of slab thickness for paraffin for 14.1 MeV neutrons.

* Curve 1 was experimentally obtained by Broerse (1967).

** Curve 2 was experimentally obtained by author.

and with a shield respectively) as a function of the thickness of paraffin. The experimental results for the attenuation of neutrons by paraffin were compared with the results obtained by Broerse (1967). The results are in very good agreement with the attenuation curve obtained by Broerse. The relatively small variations can be attributed to the differences in the hydrogen content ratio in the paraffin and to the contribution of gamma radiation to the absorbed dose. The experimental results for steel are presented in table III, and figure 11. The figure shows the equivalent transmission factor D_x/D_0 as a function of the thickness of steel. In this part D_0 was determined without any shielding and then the chamber was surrounded by borated paraffin to reduce the scattered components of the absorbed dose, and D_x was determined by attenuating the beam with steel slabs of thickness 5 cm. The results were compared with experimental data obtained by Greene (1969). It can be easily seen that the values are in good agreement with Greene's values up to a thickness of 17 cm. The sharp drop in our experimental curve beyond 17 cm may be due to scattered neutrons. In Green's experiments the chamber was not shielded by borated

Table III

Attenuation of 14.1 MeV neutrons by steel.

H.V = 80 KV, I = 400 μ A.

The ionization chamber was placed at a distance of 60 cm from the target.

Thickness of steel (cm)	Ionization current i (mV)	Proportional counter p (counts/min.)	i/p $\times 10^{-2}$	Corrected ionization current i' (mV)	Dose rate D (rad/min.)	Transmission factor D_x/D_0
0	3200	222184	1.440	3200	.336	1.00
5	1472	294441	.838	1862	.195	.59
10	1340	236209	.572	1270	.133	.40
15	758	237264	.319	708	.074	.23
20	365	393137	.093	205	.021	.06

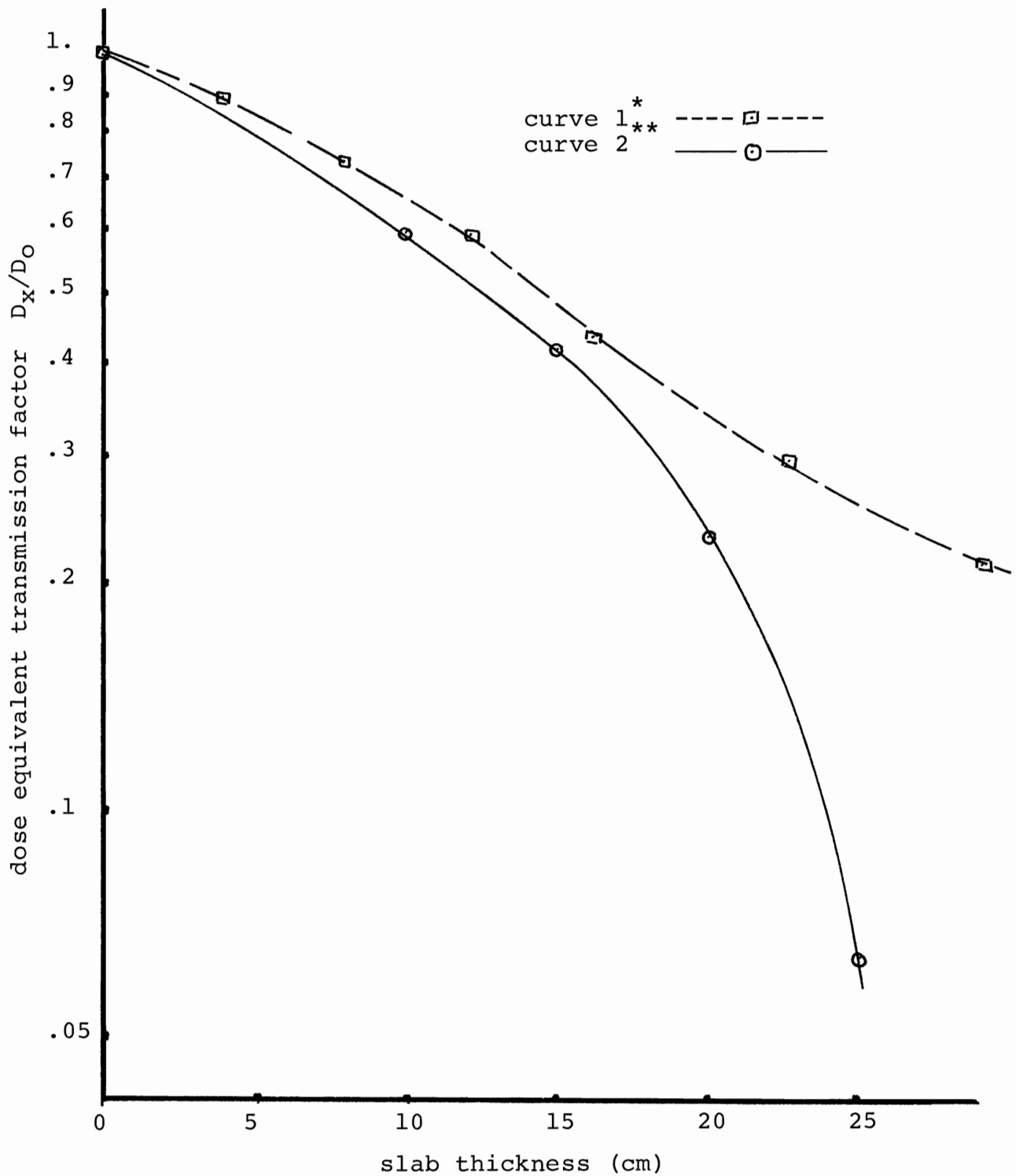


Figure 11. Relative dose equivalent values as a function of slab thickness for steel.

* Curve 1 was experimentally obtained by Greene (1969).
** Curve 2 was experimentally obtained by author.

paraffin. Since in our experiments the chamber was shielded by borated paraffin from scattered neutrons, the contribution of these neutrons to the absorbed dose was reduced and lower values for dose rate was obtained for steel thicknesses greater than 17 cm. Figure 12 shows another set of results to demonstrate the effects produced by different combinations of steel, lead, paraffin, borated paraffin, and borated water. Here the chamber was placed at a distance of 50 cm from the target and different layers of different materials were placed in front of the target to determine the transmission factor D_x/D_0 as a function of slab thickness. It can be easily seen from the curves that steel and lead are better attenuators of neutron than paraffin and borated paraffin up to a thickness of 20 cm. On the other hand, it should be noted that the differences between the slope of the steel and the borated paraffin diminish for a thickness of attenuator greater than 20 cm. This shows that borated paraffin is as efficient as steel for these thicknesses. In other words steel is a very good attenuator for fast neutrons but borated paraffin may be more efficient in this region since the neutrons were slowed down. Concerning attenuation characteristics of borated water, it should be noted that the attenuation curve

Table IV

Transmission of different combinations of different materials.

H.V = 80 KV, I = 400 μ A.

The ionization chamber was placed at a distance of 60 cm from the target.

Nature of the material	Thickness of the material (cm)	Ionization current i (mV)	Proportional counter p (counts/min.)	i/p	Corrected ionization current i' (mV)	Transmission factor D_x/D_0
-	-	5430	21301	.255	54300	1.00
Borated paraffin	10	4810	28395	.169	3598	.66
Lead	5	2835	31208	.090	1917	.35
Paraffin	4	2310	29985	.077	1640	.30
Paraffin	4	1844	27578	.067	1427	.26
Paraffin	4	1480	25074	.059	1256	.23
Borated paraffin	8	640	23369	.027	575	.10
Steel	2	566	27970	.020	426	.08
Steel (1 cm) + Borated paraffin + (14 cm) + Water (20 cm) + Lead (5 cm)		675	38896	.022	488	.09

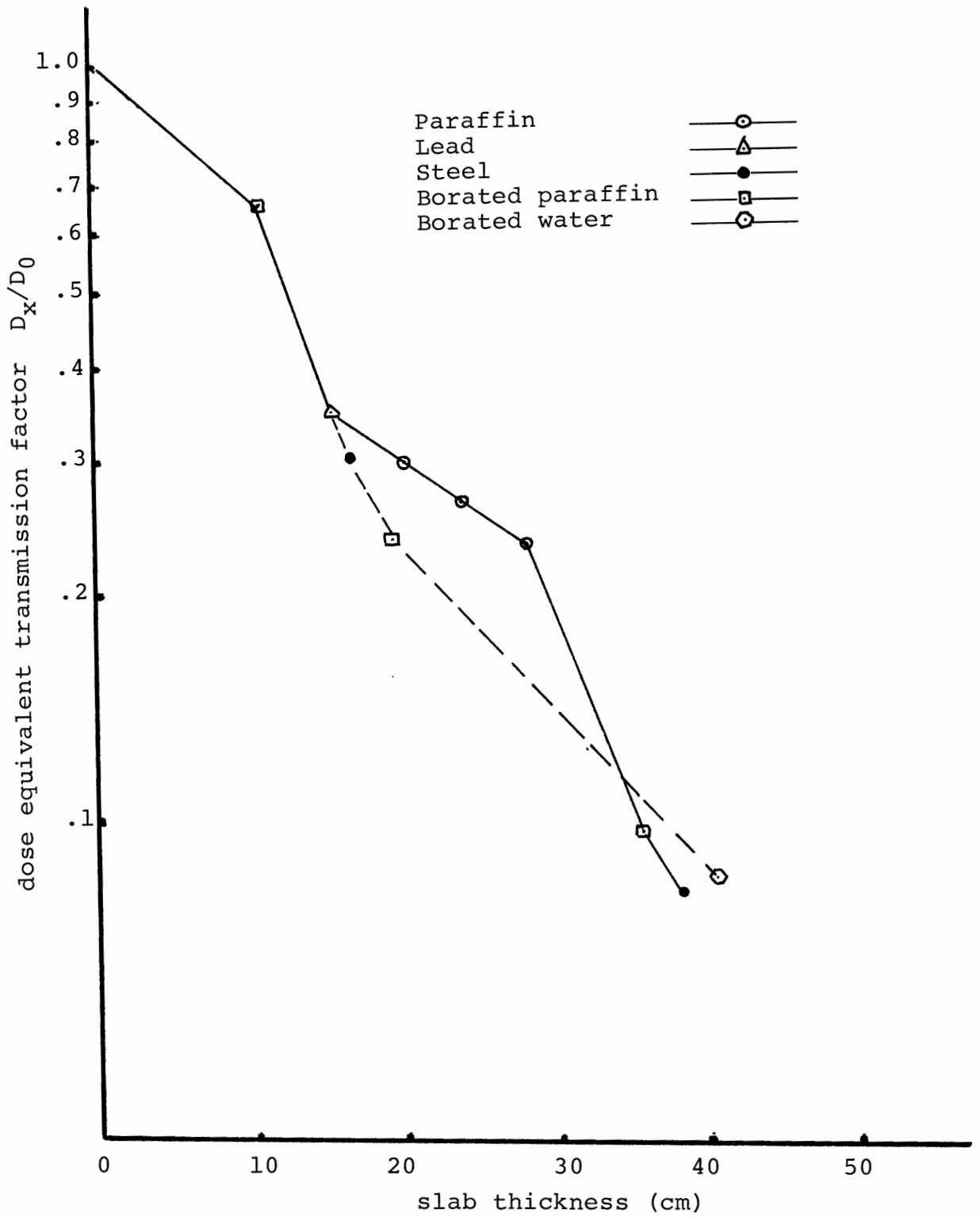


Figure 12. Relative dose equivalent values as a function of different thicknesses of different materials.

of the borated water has almost the same slope as that of paraffin.

In figures 13 and 14 the change of the dose rate as a function of the distance of the ionization chamber from the target was studied without and with a steel shielding respectively. The dimensions and the shape of the shielding is shown in figure 15 . The position of the ionization chamber was changed in steps of 10 cm to determine the corresponding dose rate. The sudden increase of the dose rate for a distance less than 10 cm indicates the contribution of gamma-rays from the shielding around the target. In figure 14 there is a greater contribution of gamma-rays because of the steel shielding. The change in slope of the curve obtained in the figure 14 compared to that of figure 13 may be attributed to: Firstly, to the contribution of gamma-rays from excited levels of steel and from the activated steel by 14.1 MeV neutrons. Secondly, to the contribution of scattered neutrons escaping from the steel shield and scattered neutrons from the wall.

Since the main requirement to be considered in designing a shield and a collimation system for radiotherapy unit is the need for minimum transmission of any radiation besides the useful beam, the posi-

Table V

Change of dose rate as a function of the distance of the ionization chamber from the target.

H.V = 80 KV, I = 400 μ A.

Distance from target (cm)	Ionization current i (mV)	Proportional counter i/p	Corrected ionization current i' (mV)	Dose rate D (rad /min.)	Transmission factor D_x/D_0
10	27500	38325	27500	2.887	1.00
20	22800	96339	9060	.951	.33
30	9500	72022	5054	.530	.18
40	6500	81229	3065	.321	.11
50	4400	79722	2107	.221	.08
60	3350	79428	1617	.169	.06

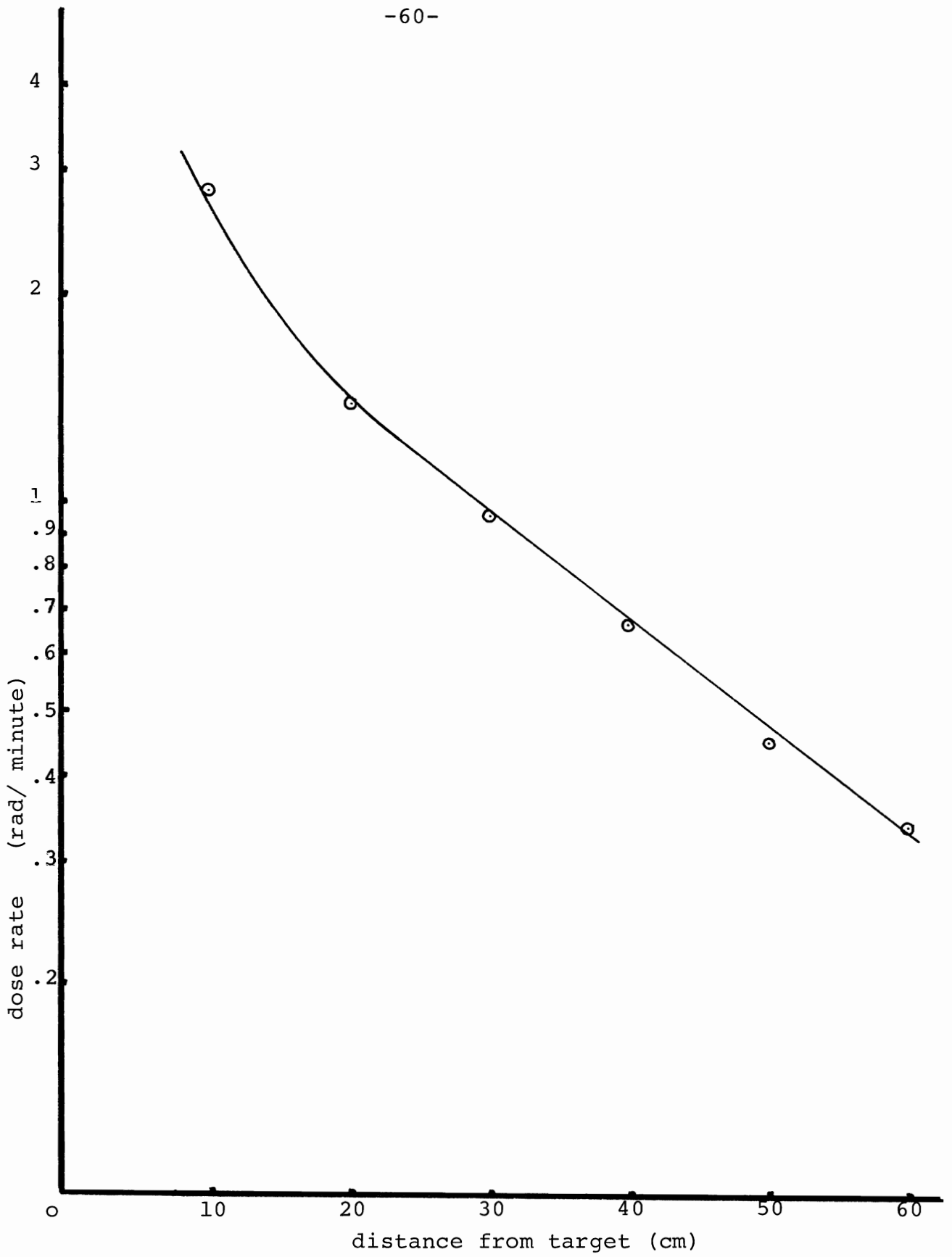


Figure 13. Dose rate as a function of distance from target.

Table VI

Change of dose rate as a function of the distance of the ionization chamber from the target with steel shielding

H.V. \approx 80 KV, I \approx 400 μ A.

Distance from target (cm)	Ionization current i (mV)	Proportional counter p (counts/min.)	i/p	Corrected ionization current i' (mV)	Dose rate D (rad/min.)	Transmission factor D_x/D_0
0	1975	4353	.453	1975	.207	1.00
5	1503	4138	.358	1560	.163	.81
10	1330	3937	.337	1469	.154	.77
14	1145	3868	.295	1286	.135	.68

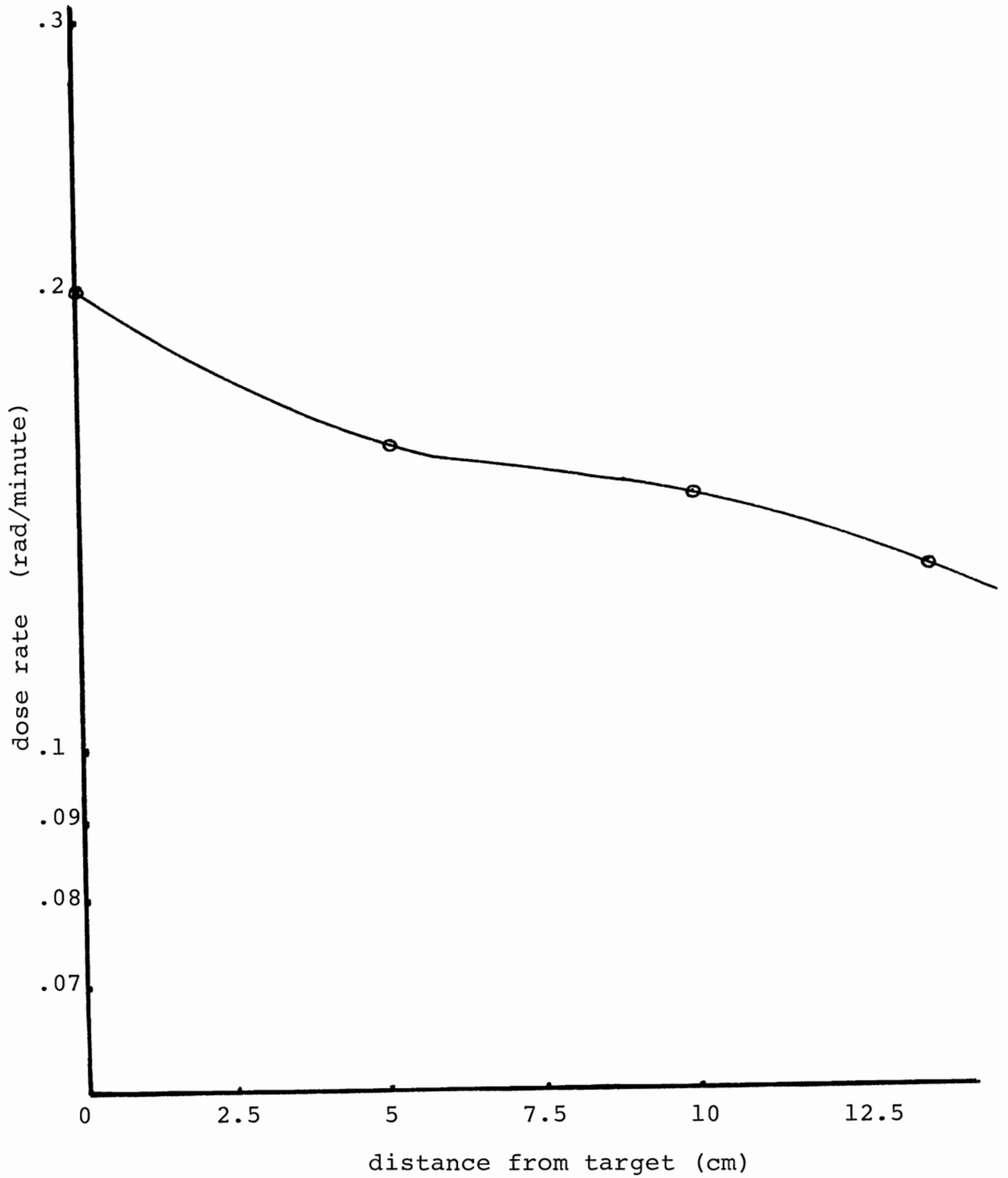


Figure 14. Dose rate as a function of distance from target with steel shielding.

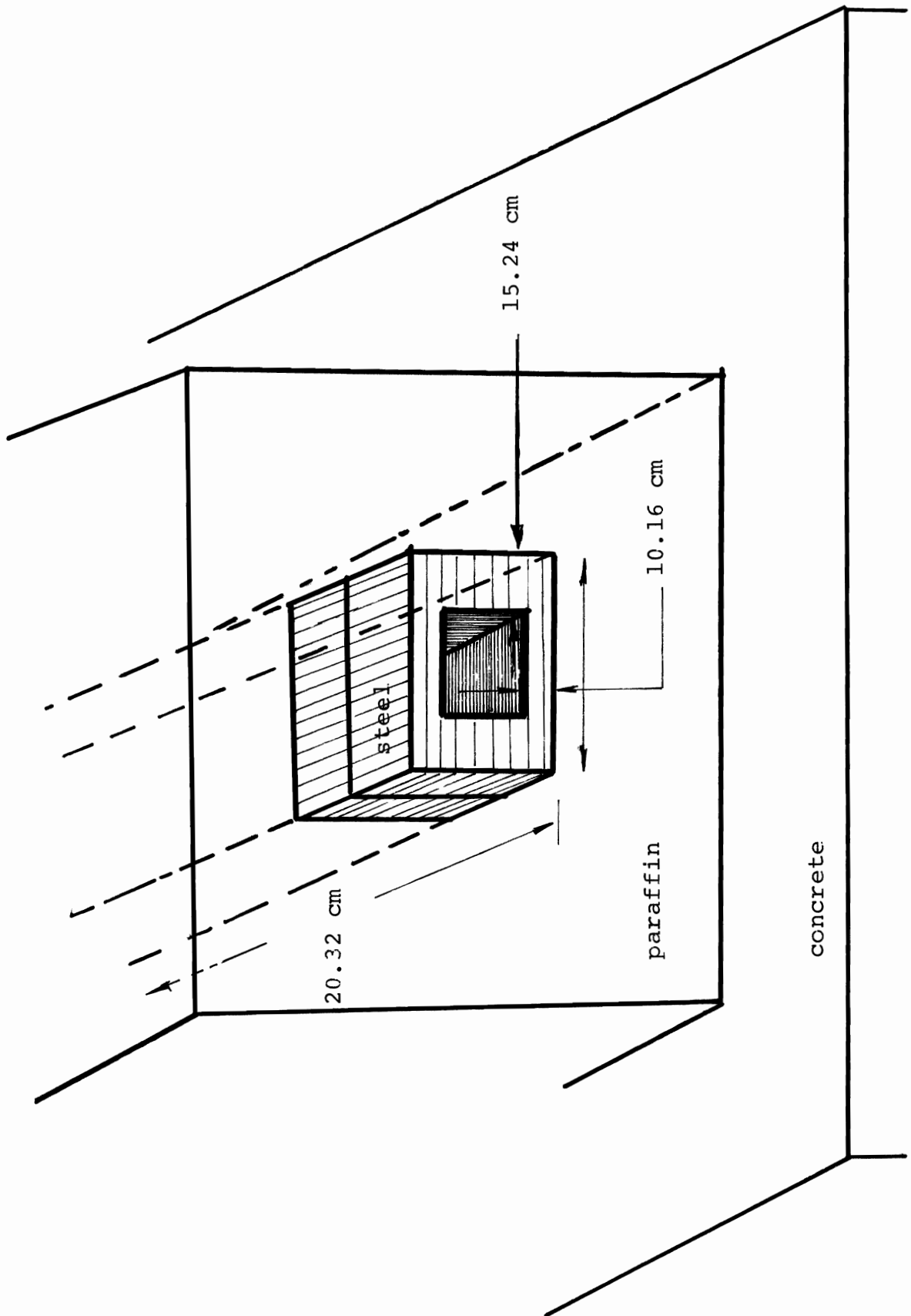


Figure 15. Dimensions and shape of the shielding.

tion of the ionization chamber was changed parallel to the shielding in front of the beam and the intensity of the beam in arbitrary units as a function of position was recorded by the electrometer and a recorder (see figure 16). It can be seen that the collimator reduces the intensity of neutron beam to a few percent of the forward maximum which is quite acceptable.

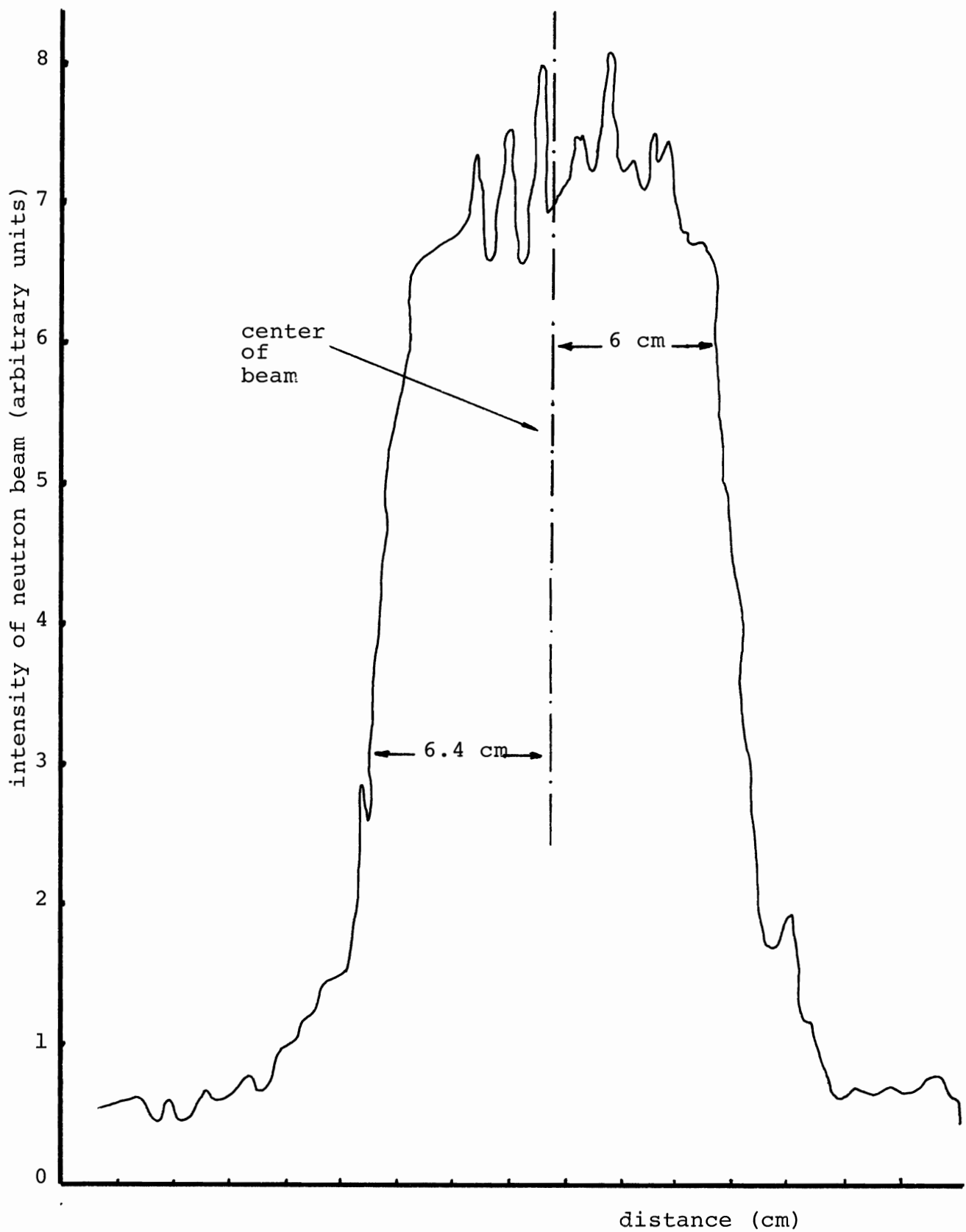


Figure 16. A "scan" made across the center of the neutron beam.

CHAPTER VI

CONCLUSION

The object of the research described was to study the attenuation and absorption of fast neutrons. Although this work is mainly concerned with the attenuation and collimation of neutrons, the initial attempts to determine the dose rate produced by the neutron generator are included.

From the results and our data given in tables I, II, and III, it can be concluded that steel appears to be the one of the most suitable materials for the collimation of 14.1 MeV neutron beams. From the families of curves as presented in figures 10, 11, and 12, it seems that a shield for fast neutron source should consist of an inner core of steel from 20 cm to 30 cm thick serving to attenuate primary neutrons, followed by a layer of paraffin or borated paraffin. This layer is less efficient than steel in stopping the remaining primary neutrons but is as efficient in stopping scattered neutrons. This is clearly shown when the attenuation data of Green is compared with those in this thesis. An outer layer of steel or lead may be used to absorb gamma-rays

generated from the capture of neutrons in paraffin or in borated paraffin and from the steel shielding itself.

REFERENCES

1. Aebersold, P.C., Anslow, G.A., Phys.Rev., 69,1,1946.
2. Anglinzew, K.K., Dosiometrie Ionisierender Strahlung VEB, Deutscher Verlag der Wissenschaften, Berlin, 18,142,1961.
3. Baarh, J., Sullivan, A.H., Phys.Med.Biol. 2,269,1969.
4. Barendsen, G.W., Int.J.Radiat.Res., 8,453,1964.
5. Beckurts, K.H., Wirtz, K., Neutron Physics. Springer Verlag New York Ins., 1964.
6. Berry, R.J., Andrews, J.R., Brit.J.Radiol., 36,49,1963.
7. Bewley, D.K., Brit.J.Radiol., 38,613,1963.
8. Bewley, D.K., Radiology, 86,251,1966.
9. Bewley, D.K., Hornsey, S., Biological Effects of Neutron and Proton Irradiations. Vol.II, International Atomic Energy Agency, Vienna, 1964.
10. Bewley, D.K., Parnell, C.J., Proceedings of the XI th International Congress of Radiology., 1965.
11. Bewley, D.K., Parnell, C.J., Brit.J.Radiol., 42,281,1969.
12. Bewley, D.K., Mc Nally, N.J., Brit.J.Radiol., 42,289,1969.
13. Boag, J.W. Radiat.Res., 1,323,1954.
14. Broerse, J.J., Effects of Energy Dissipation by Monoenergetic Neutrons in Mammalian Cells and Tissues. Radiobiological Institute TNO, Rijswijk (Z.H.), the Netherlands, 19.
15. Broerse, J.J., Ammers, H.V., Int.Rad.Biol., 10,5,417,1965.

16. Broerse, J.J., Barendsen, G.W., IAEA Symposium on Biological Effects of Neutron and Proton Irradiations, 1, 309, 1964.
17. Broerse, J.J., Werven, F.J., Hlth.Phys., 12, 83, 1966.
18. Coon, J.H., Fast Neutron Physics., Interscience Publishers, New York, 1960.
19. Fowley, J.L., Brolley, J.E., Rev.Mod.Phys., 28, 103, 1956.
20. Fowley, J.L., Morgan, R.L., Brit.J.Radiol., 36, 422, 1963.
21. Graves, E.R., Davis, R.W., Phys.Rev., 97, 1205, 1955.
22. Gray, L.H., Brit.J.Radiol., 10, 721, 1937.
23. Greene, D., Thomas, R.L., Phys.Med.Biol., 14, 45, 1969.
24. Greene, D., Thomas, R.L., Brit.J.Radiol., 41, 455, 1968.
25. Greene, D., Nature, 202, 204, 1964.
26. Hewitt, H.B., Brit.J.Cancer, 13, 675, 1959.
27. Hurst, G.S., Brit.J.Radiol., 27, 353, 1954.
28. ICRU Report, Radiation Quantities and Units, 10 a, National Bureau of Standards, Handbook 84, 1962.
29. ICRU Report, Physical Aspect of Irradiation, 10 b, National Bureau of Standards, Handbook 85, 1964.
30. ICRU Report, Radiobiological Dosimetry, 10 c, National Bureau of Standards, Handbook 88, 1963.
31. ICRU Report, Measurements of Absorbed Dose of Neutrons and of Mixtures of Neutrons and Gamma Rays, National Bureau of Standards, Handbook 75, 1961.
32. ICRU Report, Protection Against Radiations from Sealed Gamma Sources, National Bureau of Standards, Handbook 73, 1960.

33. ICRU Report, National Bureau of Standards, Handbook 62, 1956.
34. Kaplan, I., Nuclear Physics., Addison-Wesley Publishing Company, Inc., London, 1964.
35. Landau, L., J.Phys., (U.S.S.R.), 8, 201, 1944.
36. Langsdorf, A., Fast Neutron Physics. Interscience Publishers, New York. 1960.
37. Muller, J.H., Science, 66, 84, 1927.
38. Randolph, M.L., Radiat, Res., 7, 47, 1957.
39. Read, J., Brit.J.Radiol., 25, 651, 1952.
40. Rhody, B.R., Hopkins, J.I., Radiat. Res., 2, 523, 1955.
41. Rosemary, T.B., Radiat. Res., 15, 1, 1961.
42. Rossi, H.H., Rosenzweig, W., Radiat. Res., 2, 417, 1955.
43. Rossi, H.H., Radiat. Res., 10, 522, 1959.
44. Rossi, H.H., Radiat. Res., suppl., 2, 290, 1960.
45. Rossi, H.H., Failla, G., Neutrons Dosimetry., Medical Physics, Vol II, The year book publishers, Inc., Chicago, 1960.
46. Rossi, H.H., Radiation Dosimetry, Academic press, 1956.
47. Rossi, H.H., Bateman, J.L., Radiat. Res, 13, 503, 1960.
48. Rossi, H.H., Nucleonics, 21, 7, 75, 1963.
49. Smith, J.R., Phys. Rev., 95, 730, 1927.
50. Shonka, F.R., Rose, J.E., and Failla, G., Second United Nations International Conference on the Peaceful Uses of Atomic Energy., conf. paper p 753, 1958.